TOPICAL REVIEW

Spectroscopic studies with the use of deep-inelastic heavy-ion reactions

INSTITUTE OF PHYSICS PUBLISHING JOURNAL OF PHYSICS G: NUCLEAR AND PARTICLE PHYSICS

J. Phys. G: Nucl. Part. Phys. **32** (2006) R151–R192 doi:10.1088/0954-3899/32/6/R01

TOPICAL REVIEW

Spectroscopic studies with the use of deep-inelastic heavy-ion reactions

R Broda

Niewodniczański Institute of Nuclear Physics PAN, Kraków, Poland

Received 6 February 2006
Published 12 May 2006
Online at stacks.iop.org/JPhysG/32/R151

Abstract

Gamma spectroscopic studies exploiting deep-inelastic heavy-ion reactions in thick target experiments are reviewed. The description of physical motivation, history of early experiments, analysis of the N/Z equilibration process as well as the outline of the experimental method and data analysis are followed by the presentation of main results obtained in various regions of the nuclide chart. Brief comments on thin target spectroscopy experiments involving fragment detection and future outlook are summarized.

1. Introduction

A wealth of information on the structure of neutron-deficient nuclei has been accumulated in many years of advanced spectroscopic studies which exploited standard heavy-ion fusion evaporation reactions. This convenient way to produce new nuclei allowed us to investigate them in a broad range of spin and excitation energies, reaching also nuclei located in very exotic regions close to the proton drip line. On the other hand, the neutron-rich nuclei are much more difficult objects to reach for in-beam spectroscopic study and the structural information was for a long time limited to mainly those properties which could be examined in radioactive decays. Even the nuclei located at the neutron-rich edge of the beta stability valley are mostly inaccessible in fusion–evaporation reactions and consequently their yrast structures remained hitherto largely unknown. In fact, the neutron-rich nuclei can be produced only with the use of complex nuclear reactions, which require application of very selective techniques and highly efficient detection systems to exploit reaction channels characterized by low cross sections. Apparently, also the future use of radioactive beams will not significantly change the situation, and binary reactions must be viewed as the main technique to reach more exotic species in the neutron-rich region of nuclei.

Experimental efforts to reduce this apparent asymmetry of information in the chart of nuclides were further motivated by the growing interest in studying the nuclear structure as a

function of isospin, consequently reaching isotopes with neutron excess as large as possible. Qualitatively new features of nuclear structure and interesting phenomena are expected from theoretical considerations of these large size, weakly bound nuclei with the diffused surface composed mostly of neutrons e.g. [1–3]. Modified average nuclear potential as well as isospin-dependent components of effective interactions can change the shell structure dramatically, which according to various predictions may lead to the quenching of shell effects, but in some cases also to the occurrence of new magic numbers. Experimental attempts to enter this exotic region of nuclei with spectroscopic studies were therefore strongly stimulated by theoretical expectations. For the sake of controlled progress in understanding the structural changes it is rather obvious that such attempts should also include less exotic nuclei located much closer to the beta stability valley.

The construction of large gamma multi-detector arrays, which allowed us to collect high-quality and high-statistics gamma coincidence data paved the way to spectroscopic studies of many nuclei that could not be accessed in standard fusion–evaporation reactions. The essential breakthrough came from the fact that the very complicated and previously untreatable gamma spectra accompanying complex nuclear processes could now be resolved due to the selectivity obtained in the detailed gamma coincidence analysis. Already the operation of the first moderate size gamma detector arrays allowed us to initiate fruitful studies of nuclei produced in spontaneous fission and in deep-inelastic heavy-ion reactions (DIHIR). In both processes the large number of excited reaction products emit gamma radiation and contribute to the total gamma spectrum of extreme complexity. With the new data quality such spectra could be resolved in both cases by using almost identical methods of gamma coincidence analysis. Following the rapid progress in the construction of large gamma detector arrays, the spectroscopic studies exploiting spontaneous fission and DIHIR were developed in parallel efforts and became the main source of new information on many previously unknown neutron-rich nuclei.

A detailed description of techniques used in spontaneous fission spectroscopy is given in the review by Ahmad and Phillips [4]. The mass distributions of nuclei produced in the spontaneous fission of the ^{252}Cf or ^{248}Cm isotopes, which are usually used in such measurements, define the region of nuclei which can be reached in the analysis. The simplicity of measurements with the use of radioactive sources allowed us to accumulate very high statistics coincidence data which included gammas from very neutron-rich nuclei produced with very small production yields down to 0.1% per fission event. Moreover, relatively easy identification procedures of new nuclei, based on the observation of gamma coincidences with the known gamma transitions from the accompanying fission fragments, contributed to the rapid flow of information on detailed level schemes of many nuclei. The obtained results included new regions of deformed nuclei which could be studied up to fairly high-spin ranges, e.g. [5, 6] as well as spherical shell model nuclei in the neutron-rich region of the doubly magic ^{132}Sn, e.g. [7–9], where a uniquely complete spectroscopy provided essential experimental input for shell model studies. Although the technique of gamma coincidence data analysis used in a parallel development of spectroscopic studies exploiting DIHIR is nearly identical, there are many differences in the practical application of both methods for the spectroscopy of hard-to-reach nuclei. These differences and the generally more demanding experimental approach will become transparent in the present review of gamma spectroscopic studies with deep-inelastic heavy-ion reactions. In the next two sections a brief outline of experiments which initiated such research will be followed by the summary of efforts devoted to investigate the most important features of the DIHIR for spectroscopic applications. The essential part of this review will describe the most characteristic results obtained in various regions of the chart of nuclides.

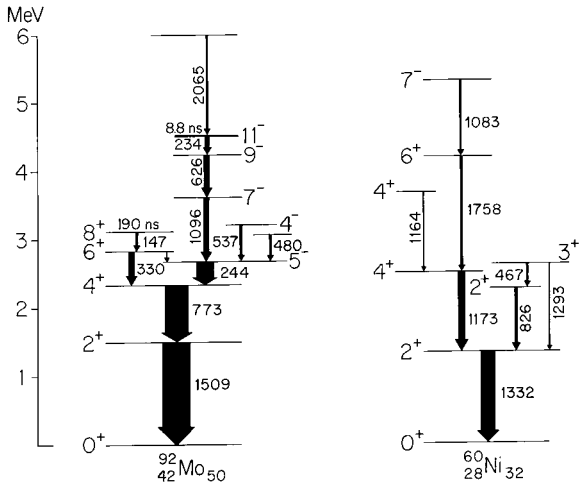

Figure 1. Population (transition arrow thickness) of states observed in the ^{92}Mo-target and ^{60}Ni-beam nuclei in deep-inelastic collisions [10].

2. First experiments and the outline of the experimental method

In 1988 at the Argonne National Laboratory the ^{92}Mo + 255 MeV ^{60}Ni gamma coincidence experiment was performed originally aimed at elucidating high-spin level structures of neutron-deficient $N = 82$ isotones produced in the fusion–evaporation reaction. The enriched 0.8 mg cm^{-2} ^{92}Mo target backed with thick Pb was placed in the centre of 12 Compton-suppressed Ge detector array and in a three day run excellent gamma–gamma coincidence data were acquired. In the subsequent analysis of gamma coincidences, apart from the fusion–evaporation residues, the data were found to also include many events arising from inelastic and transfer reaction products. A thorough analysis of these events provided unexpectedly unique information on 13 binary reaction channels which could be identified from the data by recognizing known gamma transitions emitted from the excited final nuclei [10]. Important observations were made, which pointed out the potential attractiveness of these lines of investigation when in the future much larger gamma-ray detector arrays become available. Firstly, the population of high-spin (up to $I = 12$) non-collective states was observed, along with the high excitation energy transfer which sometimes led to subsequent neutron emission. Figure 1 shows the observed population of known states in the ^{92}Mo-target and ^{60}Ni-beam nuclei which indicated the possibility of using deep-inelastic reactions for yrast spectroscopy. Secondly, the cross-coincidences between gammas emitted from two excited nuclei appearing in the reaction exit channels could be easily established. The latter feature was recognized as a potential tool to study correlated energy and angular momentum transfers into both product nuclei and also as a possible way to identify gammas from unknown nuclei by establishing their reaction partners in the exit channel. Consequently a specific application of such an analysis for the spectroscopy of unknown yrast structures in neutron-excessive nuclei was suggested [10].

The subsequent experiment testing the potential application of this technique was performed with the OSIRIS multi-detector array at the HMI Berlin, using the ^{54}Fe beam of 255 MeV energy and the 1.2 mg cm^{-2} ^{106}Cd target backed with a thick ^{208}Pb layer [11]. The collected gamma coincidence data were analysed in a most complete way and covered practically all spectra of events arising from various nuclear processes taking place at 30 MeV above the Coulomb barrier collisions of ^{54}Fe and ^{106}Cd nuclei. The use of beam pulsing

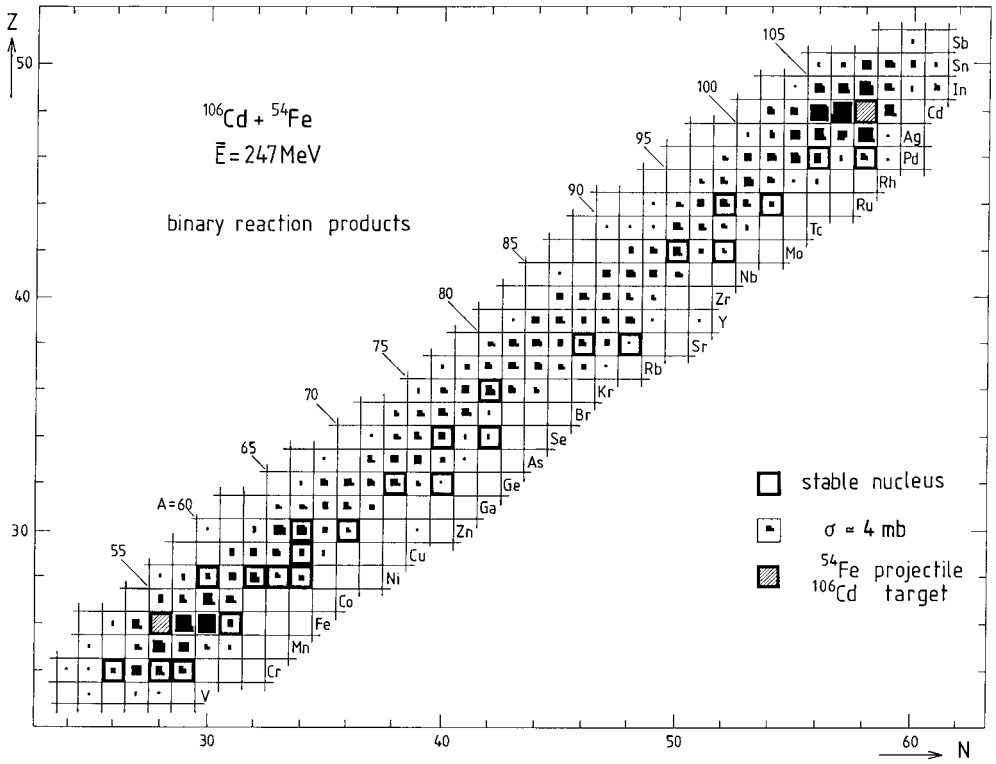

Figure 2. Production cross sections for binary reaction products in ^{54}Fe + ^{106}Cd collisions. In the same experiment cross sections for fusion–evaporation products were determined. Reprinted with permission from [11] © 1994 American Physical Society.

with the repetition time of 300 ns allowed us to separate prompt and delayed events which helped us to analyse quantitatively isomeric and short-lived radioactive decays; supplementary measurements and analysis of the long-lived radioactive products were also performed. As a consequence a nearly complete distribution of final products could be established by gamma analysis and yielded cross sections for exclusive channels of fusion–evaporation, fusion–fission, quasi-elastic transfer and deep-inelastic transfer reactions (figure 2). The variation of the average N/Z ratio extracted for each mass is shown in figure 3 along with the obtained mass distribution for all binary reaction products. In a more laborious analysis the population of different spin states was extracted. Diagrams shown in figures 4(a) and (b) represent the side feeding of states observed in target-like nuclei and their most probable complementary beam-like fragments. One may note that even for nuclei differing by only a few nucleons from the initial ones a strong population of a few selected states in quasi-elastic reactions is accompanied by a long tail of high-spin population. This high-spin population then becomes a dominant feature for products involving large transfer of mass. However, the most spectacular result was the heavy and light fragment correlation diagram (figure 5) obtained from the detailed analysis of gamma cross-coincidences. The choice of the colliding nuclei simplified such an analysis since practically all nuclei produced in binary reactions fall in the region easily accessible for spectroscopy and were well known from earlier spectroscopic studies. Points included in the diagram and located on lines corresponding to the summed mass numbers of both correlated products mark all cases for which the simultaneous appearance of two specific nuclei in the exit channel could be established by observed gamma coincidences. Whereas the 11 points

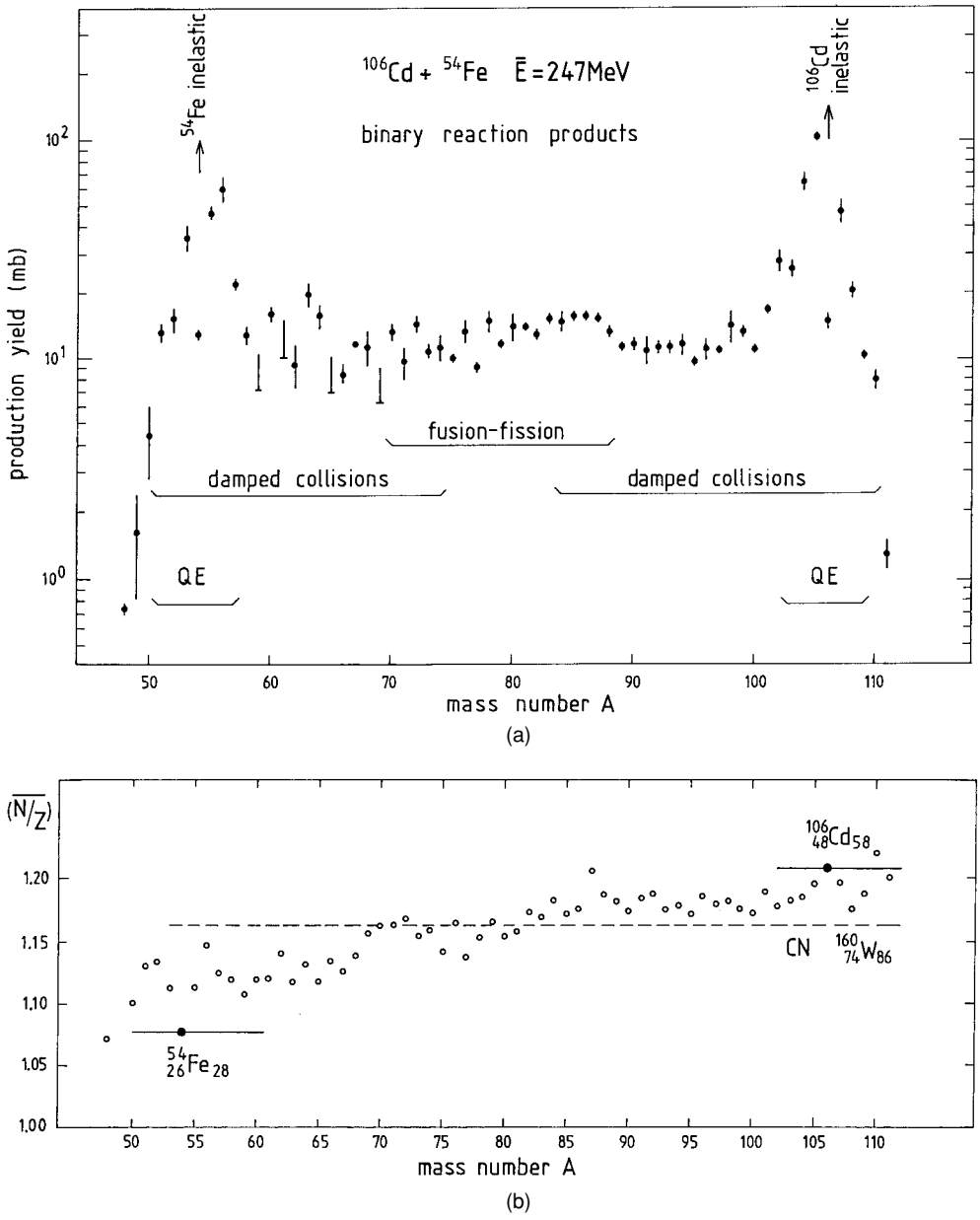

Figure 3. Isobar-integrated production cross sections (a) and the average N/Z ratios (b) as a function of binary reaction product mass in ^{106}Cd + ^{54}Fe collisions. Reprinted with permission from [11] © 1994 American Physical Society.

located on the $A = 160$ line indicate reaction channels not involving any particle evaporation, all others correspond to secondary proton or neutron evaporations from the excited primary reaction products. The set of results obtained in this experiment [11] demonstrated that one is able to perform a very complete analysis of the gamma coincidence data and such a method can be successfully used for spectroscopic studies of new, hitherto unknown nuclei.

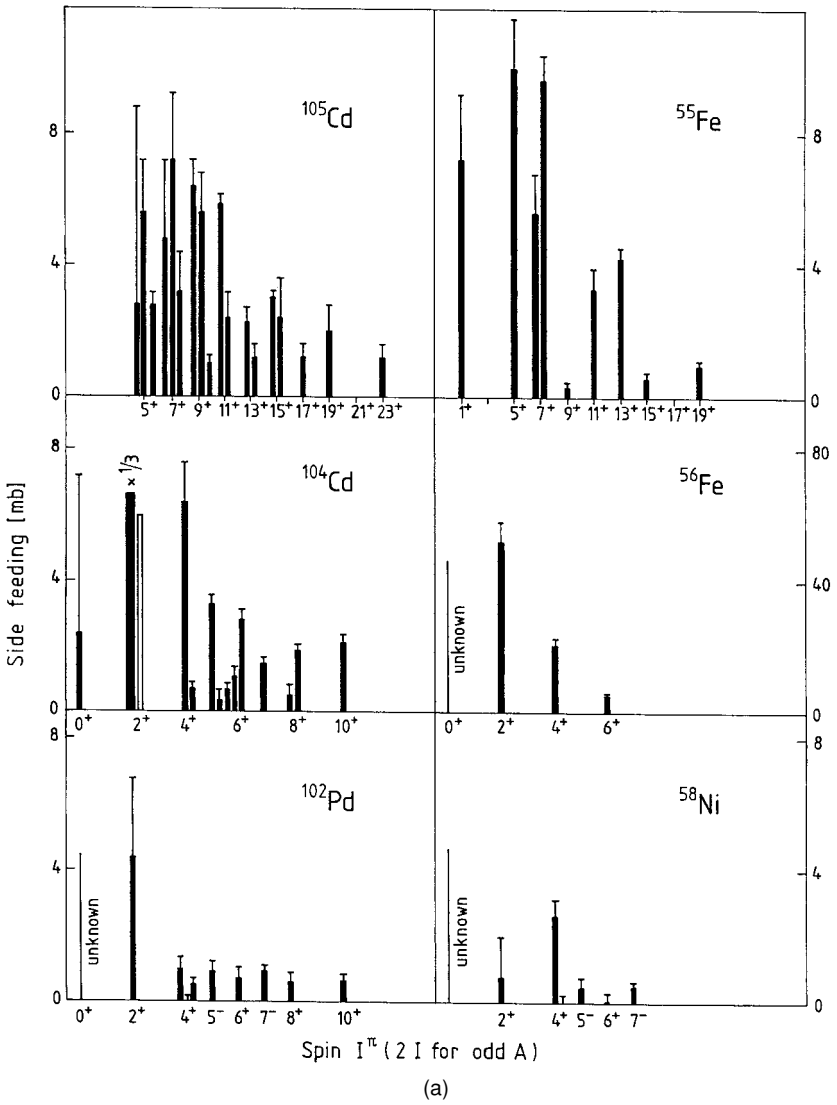

Figure 4. (a), (b) Side feeding population of various spin states for complementary binary reaction products in ^{106}Cd + ^{54}Fe collisions.

Essentially in all other experiments described in this review the neutron-rich nuclei were selected as target and beam materials in order to reach as far as possible the unknown neutron-rich isotope region. It seems appropriate to summarize now the most important points of the experimental method which is guided by the above-described initial observations [10, 11].

Figure 6 illustrates a simple classification scheme of processes taking place when two heavy nuclei collide at energies above the Coulomb barrier. The detailed description of these processes is given in review articles of Bromley's edition of Treatise on Heavy Ion Science [12]. In the most peripheral collisions, shown on the top, quasi-elastic reactions take place and the two weakly excited final nuclei arising in the reaction exit channel are identical or very similar to the initial target and beam nuclei. The processes include Coulomb excitation, nuclear

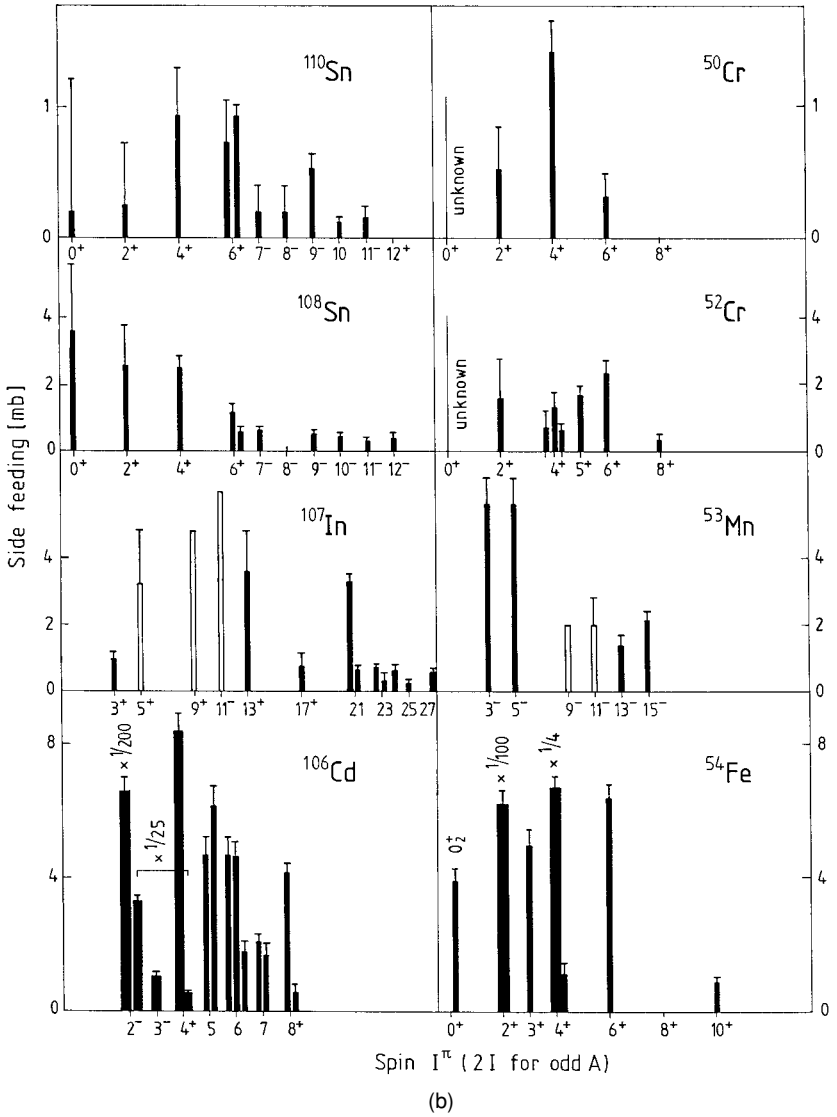

Figure 4. (Continued.)

inelastic scattering and few nucleon transfer reactions populating a small number of selected states which decay by single gamma transitions or low multiplicity gamma cascades. In central collisions shown below, the fusion reaction produces the compound nucleus with high angular momentum and well-defined high excitation energy released by subsequent evaporation of particles and high multiplicity cascades of gamma rays. The limited number of final nuclei are produced with large cross sections and for many colliding systems this process contributes predominantly to the observed gamma spectra. At limiting values of angular momentum the compound nucleus cannot sustain the rotation and undergoes fission. This fusion–fission reaction produces two fragments broadly distributed around the symmetric splitting of the mass of the compound nucleus. As both primary fragments are highly excited the secondary particle evaporation is followed by gamma emission characterized often by fairly large total

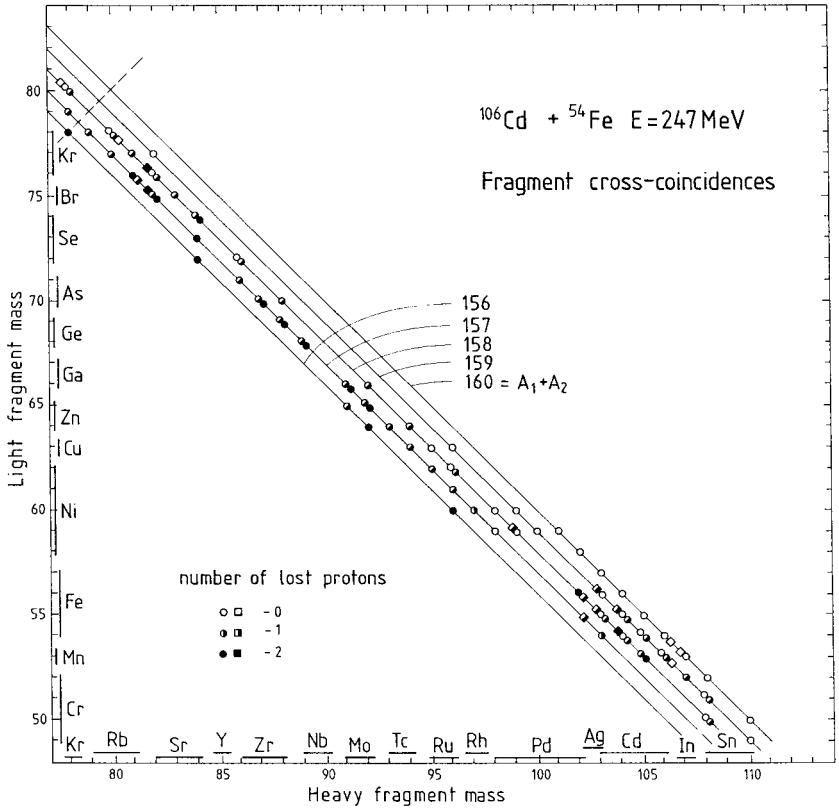

Figure 5. Correlation of light and heavy fragments established in ^{106}Cd + ^{54}Fe binary reactions. Each experimental point marks the positive identification of the simultaneous appearance of two products in the reaction exit channel by the observation of gamma cross-coincidences. For a detailed explanation see [11]. Reprinted with permission from [11] © 1994 American Physical Society.

multiplicity of correlated gamma cascades. The most important processes for the spectroscopy of hard-to-reach nuclei are shown schematically at the bottom of figure 6 and they take place at all intermediate impact parameters between the peripheral and central collisions. During the prolonged contact of nuclear matter large transfer of mass, energy and angular momentum takes place between both colliding ions, and two products arising in the reaction exit channel might differ substantially from the initial nuclei. The complexity of these reactions is reflected by various names used to classify their specific features, e.g. damped collisions, dissipative collisions, quasi-fission, multi-particle transfer or massive transfer reactions. For the purpose of this review we shall call them deep-inelastic reactions and they provide the way to produce new nuclei which previously could not be accessed for yrast spectroscopic studies. It is worthwhile to mention that for many of the selected heavy nuclei colliding systems the fusion evaporation reaction process is practically absent. Also at energies where the extra push energy is available to form the compound nucleus its subsequent decay proceeds via fusion–fission reaction which often produces fragments located also in regions interesting for the spectroscopic analysis.

The scheme of a simple experimental setup to measure in an integrated way the coincidences of gamma radiation arising from all processes described above is shown in

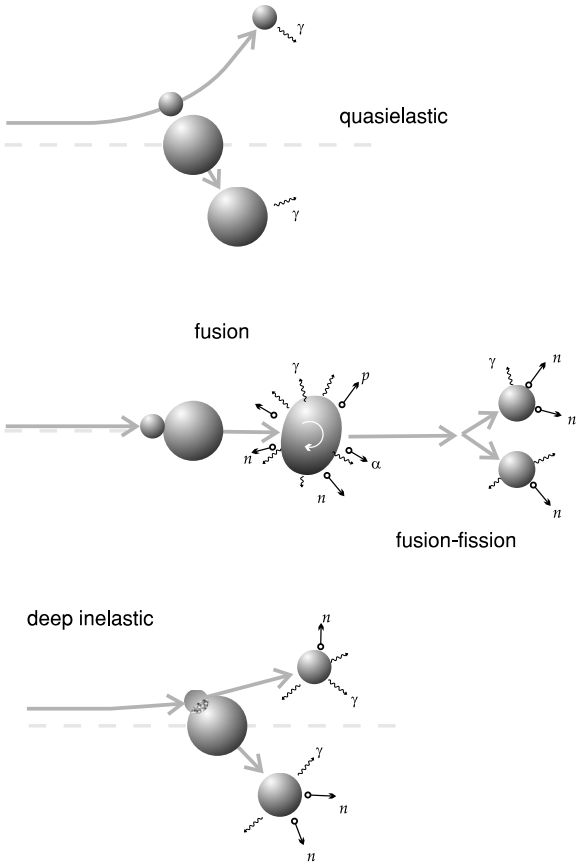

Figure 6. Schematic classification of reactions taking place in collisions of heavy ions at energies above the Coulomb barrier.

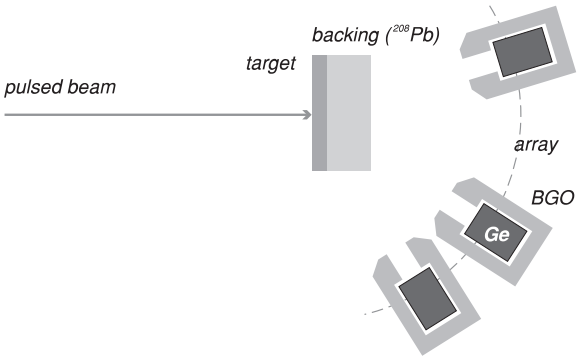

Figure 7. In the experimental setup a thick target is placed at the centre of a large germanium detector array. Gamma coincidences are measured including the lowest possible fold limited by the counting rate. Usually a pulsed beam is used.

figure 7. A thick target of selected enriched isotope (usually with ^{208}Pb backing) is located in the centre of a large gamma detector array and is bombarded with the appropriate heavy-ion beam of energy which exceeds significantly (by a factor of 1.1 to 2.0) the Coulomb barrier. All

excited reaction products arising in collisions are stopped in the target material and standard gamma–gamma coincidences are measured in a typically few days run collecting without any selectivity all events regardless of the nature of gamma emitters. In most experiments the beam pulsing (with typically 400 ns repetition time) is used to separate prompt in-beam events from those arising in isomeric and/or radioactive decays. The beam pulsing also allows us to exploit many isomeric states for a comfortably clean selection of events involving gamma transition which precede in time the isomeric decays. In a later analysis the appropriate time windows set on the delayed part of the $T_{\gamma\gamma}$ parameter enable clear identification of gamma transitions located above the isomer, as well as those which arise from the prompt cascades in the reaction partner nuclei.

The detailed analysis of the good statistics and high-quality gamma coincidence data provides the only selective power, which eventually allows us to select events originating from the previously unknown reaction products. It is important to emphasize that data analysis involves only discrete gamma lines, i.e. gamma transitions which are emitted from the stopped product nuclei. In the thick target experiments gamma transitions emitted in flight (for state and/or feeding times shorter than 1 ps) remain unobserved due to the large Doppler broadening. Practically, it turns out that most of the reaction products are populated in a spin and excitation energy range involving lifetimes longer than the stopping time and only a very few states remain undetected. Another consequence of the use of a thick target is the integration of the initial beam energy (often down to the Coulomb barrier), which is reflected in the undesired enhancement of quasi-elastic processes, e.g. Coulomb excitation. On the other hand, the integration of the reaction kinematics appears to be a welcome feature, since it allows us to also include forward scattering angles that are mostly excluded in experiments involving fragment detectors.

The gamma cross-coincidence identification procedures for transitions arising from the previously unknown nuclei will be illustrated by specific examples described in the following sections. Here, we shall briefly describe yet another of the early experiments, which in fact was the first application of the deep-inelastic heavy-ion reactions for the spectroscopy of hard-to-reach nuclei. These experiments were performed prior to the encouraging knowledge stemming from the complete analysis of the ^{54}Fe + ^{106}Cd system [11].

The physical motivation came from the earlier identification of a series of seniority 2 $(h_{11/2})^n$ isomers in neutron-deficient $N = 82$ isotones, e.g. [13, 14], which elucidated the filling of the $h_{11/2}$ proton orbital in these closed neutron shell nuclei. This phenomenon manifests itself in the spectacular variation of the B(E2) values extracted for the $10^+ \rightarrow 8^+$ isomeric transitions from the measured half-lives which assume the minimum value for the half-filled subshell. A similar study of the neutron $h_{11/2}$ orbital filling in the $Z = 50$ Sn isotopes was restricted by the lack of a suitable way to populate the expected 10^+ isomers in isotopes heavier than ^{120}Sn. The apparent prospects for spectroscopic application of deep-inelastic reactions paved the way to perform experiments in which such isomers were identified in ^{122}Sn and ^{124}Sn isotopes [15]. The experiment was exclusively devoted to search for the long-lived (in the μs range) isomers and the appropriately pulsed beam of ^{76}Ge bombarded the ^{124}Sn target backed by the thick ^{208}Pb layer with the energy exceeding the Coulomb barrier by approximately 60 MeV. The very low counting rate of gammas detected by the 12 Ge detector array in the off-beam periods enabled us to observe delayed coincidences across microsecond isomers. This gave an unambiguous identification of two crucial transitions located above the lower lying 7^- isomers and allowed us to determine half-lives of higher lying 10^+ isomers in both ^{122}Sn and ^{124}Sn isotopes. This experiment initiated the whole series of experiments exploiting deep-inelastic reactions, which provided the nearly complete systematic of such isomers in Sn isotopes as will be shown below in this review.

3. The study of the N/Z ratio equilibration process

Parallel to efforts aiming at specific spectroscopic goals, the gamma–gamma coincidence data obtained in several experiments were used to acquire more detailed information on the reaction mechanism and specifically on the N/Z equilibration process taking place during heavy-ion collisions. An extensive review of the most important features of heavy-ion reactions is given in Bromley's compilation [12] and the detailed description of damped nuclear collisions is summarized by Schroeder and Huizenga [16]. However, for the spectroscopic application aimed at the neutron-rich nuclei the most important feature of these reactions is the observed tendency to equalize the N/Z ratio between the two colliding nuclei. The direction of the proton and neutron flow taking place during the collision results in enhanced neutron transfer to the lighter reaction partner which usually has smaller N/Z ratio; for the same reason the transfer of protons to the heavy nucleus is preferred. The N/Z equilibration process was studied by several groups and the most important findings were summarized by Freiesleben and Kratz [17], yet this information was too general for detailed planning of spectroscopy experiments.

The practical aim of the laborious analysis of the gamma coincidence data aimed at studying the N/Z equilibration process was to gain a direct experimental knowledge on the range of neutron excess which can be achieved for nuclear spectroscopic studies. It was anticipated that such an analysis may be useful for three main reasons: (a) the perfect A and Z identifications based on the observation of discrete gamma lines allow us to obtain nearly complete distribution of the secondary reaction products, (b) the gamma cross-coincidences enable us to control the secondary particle evaporation and thereby allow us to reconstruct the primary distributions and finally, (c) the full integration of kinematics in thick target experiments removes the need to resort to often uncertain extrapolations. Three different colliding systems were selected for this analysis: ^{208}Pb + 350 MeV ^{64}Ni represented the neutron-rich system colliding at energy below the threshold for compound nucleus formation; the nearly identical ^{208}Pb + 345 MeV ^{58}Ni system characterized by much larger difference of initial N/Z ratios was chosen for comparison and finally ^{130}Te + 275 MeV ^{64}Ni was selected to represent the neutron-rich system involving also strong fusion–evaporation and fusion–fission channels. The detailed description of the analysis and discussion of results were presented in [18–20]. Here we shall only illustrate a few of the obtained results with the outline of main conclusions.

In figure 8 an example of a secondary product distribution is shown for the ^{208}Pb + ^{64}Ni system as obtained from the complex analysis of in-beam and off-beam gamma coincidences and long-lived radioactivity measurements. The general trends in the direction of the proton and neutron flows can be easily observed indicating the production of many neutron-rich isotopes in the beam-like nuclei. The integrated fragment mass distributions obtained from the discrete gamma radiation analysis for all three systems are shown in figure 9. Both colliding systems involving Ni isotopes show predominantly deep-inelastic reaction products, also including products centred around mass $A = 100$, which arise from the subsequent fission of heavy fragments. In the ^{58}Ni case the particularly favoured proton transfer to the heavy fragment results in the production of more fissionable nuclei and one observes strong enhancement of this part. On the other hand, as expected, the ^{130}Te + ^{64}Ni system shows additionally a strong production yield for nuclei that arise in the symmetric fission of the compound nucleus. The average N/Z ratios calculated for each product mass from the experimental isobaric production yields are shown in figure 10. In all cases the tendency to equalize N/Z ratios is clearly observed for all deep-inelastic reaction products as soon as one goes away from a narrow mass range involving large contribution of quasi-elastic

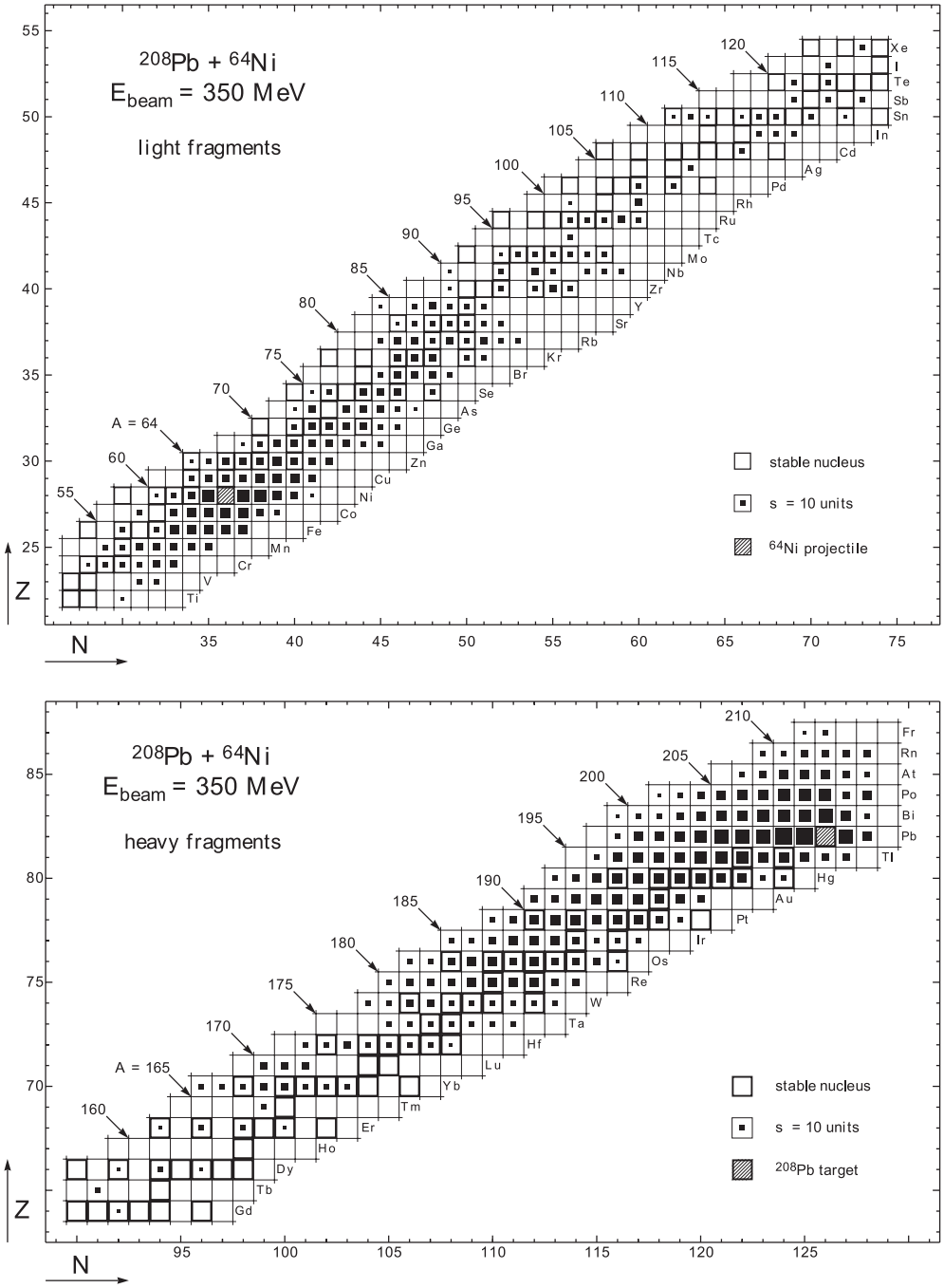

Figure 8. Distribution of heavy (a) and light (b) fragments in ^{208}Pb + 350 MeV ^{64}Ni collisions [18–20].

processes. However, this equalization is not complete, as naturally observed for the fusion–fission products in the case of the ^{130}Te + ^{64}Ni system. This result indicated an undesired limitation in the size of neutron excess which can be reached with deep-inelastic reactions for

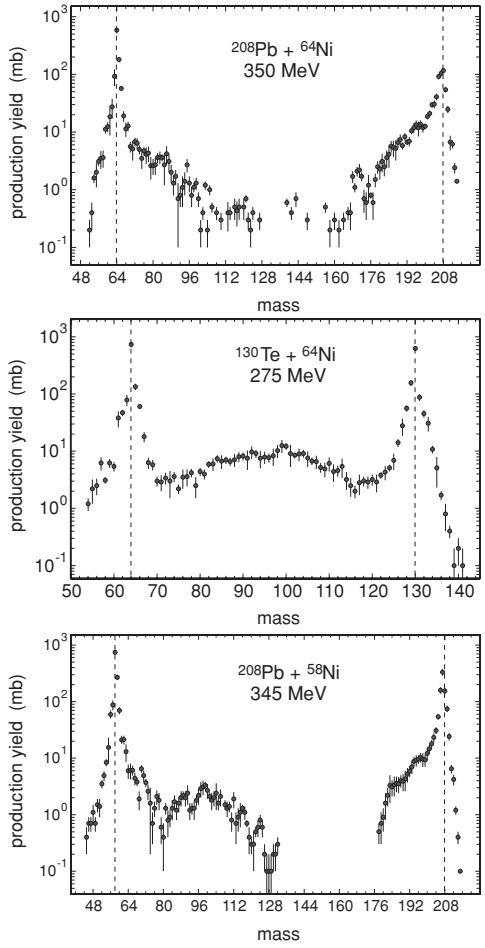

Figure 9. Isobar-integrated fragment mass distributions for three colliding systems [18, 19].

spectroscopy. Although the experimental points represent only the most probable N/Z, the distribution of isobaric product yields at each mass is not very broad and shows fast decrease for products located away from the most frequently produced isobar.

The complete treatment of these results involved the reconstruction of the primary product distributions by controlling the secondary particle evaporation with gamma cross-coincidence analysis. The resulting primary N/Z ratios were then discussed in a quantitative way, calculating the most probable N/Z ratios with the analytical formula of Świătecki [21] derived from the minimization of potential energy of two touching spheres. It became apparent that this formula overestimates the effect and the real N/Z equilibration is much less complete. Following Świătecki's suggestion [22] the formula was generalized to allow the spheres to be separated rather than touching one another, thereby simulating the effect of nuclear deformation by varying the impact of the Coulomb energy which plays a predominant role. A very satisfactory reproduction of the experimental data shown in figure 11 led to the conclusion that the N/Z equilibration process taking place in deep-inelastic reactions is strongly affected by the dynamical deformation of fragments at the scission point [18, 19].

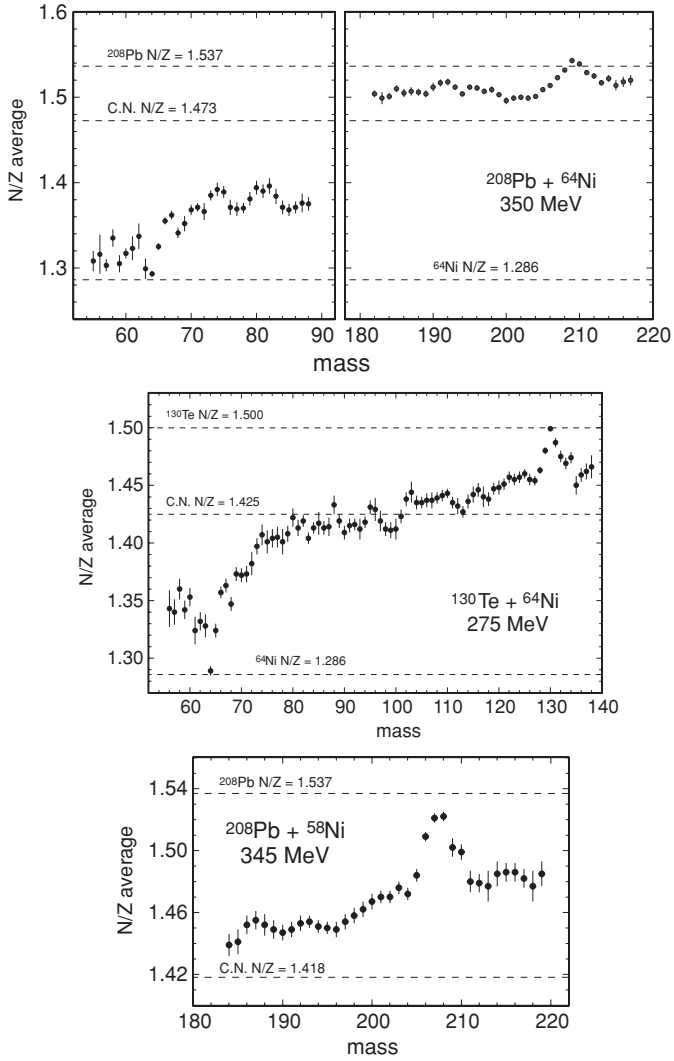

Figure 10. Mass dependence of the average N/Z ratios for isobaric products of binary reactions observed in three colliding systems [18, 19].

In many years of spectroscopic applications of deep-inelastic reactions detailed practical knowledge was acquired which allows us to select the optimal available colliding system for each region of nuclei aimed at spectroscopy. The complete analysis as shown in the above-mentioned examples is very laborious and in some specific cases a much more limited inspection was helpful to plan experiments [23]. Nevertheless the discrete gamma-ray analysis was demonstrated to be supplementary to other methods used to study reaction mechanisms and was helpful to conclude general features important for the spectroscopy.

In spite of some limitations outlined above, the deep-inelastic heavy-ion reactions proved to be an excellent tool for the spectroscopic study of many hard-to-reach nuclei. In the following sections a broad selection of the most interesting results concerning nuclei from various regions of the chart of nuclides will be presented.

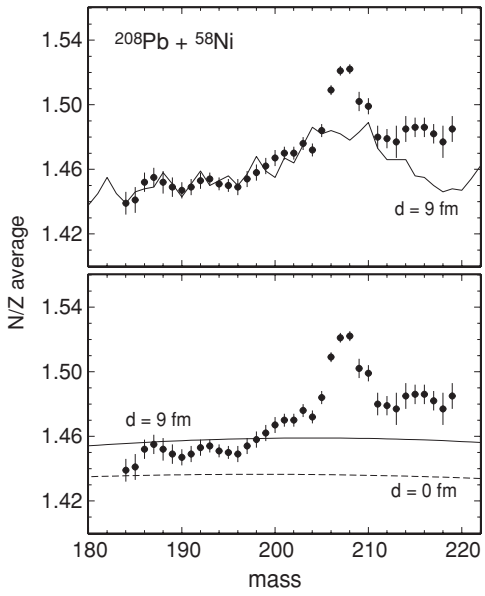

Figure 11. Comparison of the experimental N/Z results obtained for heavy fragments in ^{208}Pb + ^{58}Ni collisions with the most probable N/Z values calculated from the minimization of total energy involving experimental masses and Coulomb energy of two distant spheres connected with charged cones (above). The same results are compared with analytical formula for two distant or touching spheres (below) [18, 19].

4. Nuclear spectroscopy results

4.1. Nuclei from the spdf shells

Interesting phenomena revealed in the neutron-rich nuclei of this region can be studied theoretically within the large-scale shell model calculations which are partly guided by the hitherto available scarce experimental information. The existence of the so-called island of inversion for neutron-rich isotopes of Ne, Na, Mg [24, 25] and occurrence of new magic numbers above $N = 28$ [26] are examples of anomalies which can now be reproduced quantitatively within the shell model calculations. Any attempt to obtain new spectroscopic information on the region is therefore important to provide the desired verification of predictions and additional input to improve the theoretical approach.

One should note, however, some experimental difficulties that can be encountered in using deep-inelastic reactions for spectroscopy of these light nuclei. A strong dominance of the fusion reaction channel in collisions involving beams of light nuclei produces a high background of undesired gamma coincidence events (for very heavy nuclei targets, when the fusion evaporation reaction practically does not happen, the main source of this background arises from the fission process and from oxygen, carbon and other light impurities). Low cross sections of deep-inelastic reactions therefore demand particularly skilful analysis of the complex coincidence data. In some cases the use of the gamma multiplicity filter helps to improve the situation by selecting low gamma fold events which reduces significantly high multiplicity coincidences arising from the fusion evaporation reaction products. Another difficulty is related to the frequent occurrence of short-lived states in light nuclei, which therefore cannot be detected in thick target experiments due to the Doppler broadening of gamma lines. Usually the population pattern of these states does not provide the feeding

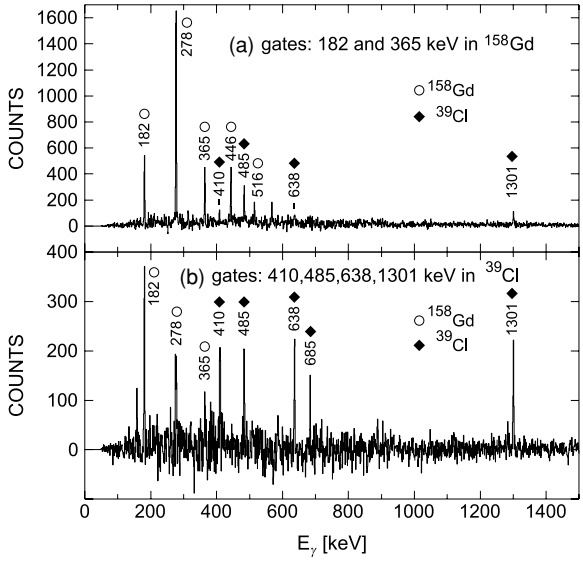

Figure 12. Gamma coincidence spectra from ^{160}Gd + ^{37}Cl experiment showing the cross-coincidence identification of transitions in ^{39}Cl arising in 2n deep-inelastic transfer. Reprinted with permission from [27] © 1994 American Physical Society.

time long enough to stop the nucleus before gamma emission and consequently the extracted spectroscopic information is much more selective than in the case of heavier nuclei.

In spite of these difficulties, already early experiments performed with very moderate gamma detector arrays yielded new results for nuclei that were previously inaccessible. A series of experiments were performed at the Argonne NL with ^{34}S, ^{36}S and ^{37}Cl beams provided by the ATLAS accelerator and ^{160}Gd targets, with the original aim to study high-spin states in Hg and Tl isotopes. The gamma coincidence data collected with the 12 detector Argonne–Notre Dame array were also used to analyse events arising in binary deep-inelastic reactions. In this way many new states were found [27] in neutron-rich nuclear products of such reactions, which gave a transparent systematic of yrast structures in ^{34}Si, ^{35}P, ^{36}S and ^{37}Cl $N = 20$ isotones, extensive comparison of high-spin states in ^{38}S, ^{39}Cl $N = 22$ isotones with shell model calculations, as well as exact location of a few states in ^{34}P and ^{33}Si $N = 19$ isotones that were studied earlier only with transfer reactions and charge particle detection techniques. Typical gamma spectra illustrating the data quality and level schemes established for $N = 22$ isotones are shown in figures 12 and 13 respectively. Later experiments performed with the GASP detector array at the INFN LN Legnaro with the ^{37}Cl beam on ^{208}Pb target allowed us to identify the new 5^- isomer in ^{32}Si and the low-lying 4^- state in the ^{32}Al isotope [28]. This was then followed by the identification of new states in ^{44}Ar and the first 2^+ state in the two-proton hole ^{46}Ar isotope [29] which was independently confirmed in a Coulomb excitation experiment with an intermediate energy radioactive beam of ^{46}Ar by the NSCL MSU group [30]. Another series of experiments performed by the UK group used deep-inelastic reactions with a ^{36}S beam and added new information on ^{36}S [31], ^{41}Cl [32] and ^{34}P [33] isotopes.

An even broader research line was initiated to study the neutron-rich nuclei located in the doubly magic ^{48}Ca region. Here the analysis was initially focused on the hitherto unknown yrast structures in ^{48}Ca itself and its closest one-particle/hole neighbours. A more demanding analysis concentrated later on the very neutron-rich products with $Z > 20$ and located further away from the core nucleus. Essentially the high-quality data from three

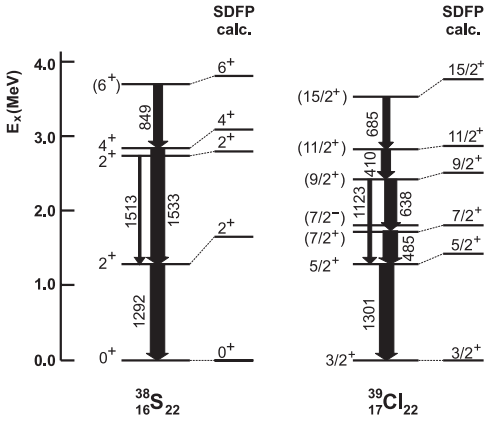

Figure 13. Level schemes of ^{39}Cl and ^{38}S established in ^{160}Gd + ^{37}Cl and ^{160}Gd + ^{36}S experiments. Reprinted with permission from [27] © 1994 American Physical Society.

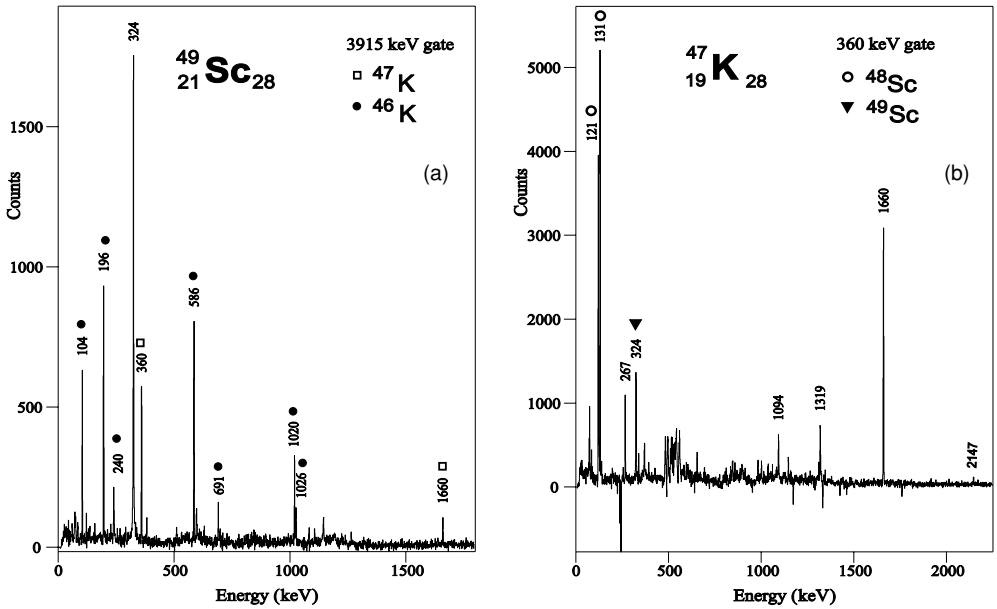

Figure 14. Gamma coincidence spectra showing the cross-coincidence transition identification in ^{49}Sc and ^{47}K from the ^{48}Ca + ^{48}Ca experiment [34, 35].

independent experiments were used for a comparative and complementary analysis which established safely yrast structures in several nuclei from this region. In all these experiments a ^{48}Ca beam of energy much above the Coulomb barrier was used to bombard thick targets of ^{48}Ca, ^{208}Pb and ^{238}U located in the centre of large gamma arrays. The experiment using the symmetric ^{48}Ca + ^{48}Ca system was performed at the INFN LN Legnaro with the GASP array and the BGO ball was used to separate in the analysis the most interesting low-fold events from the complex background arising from the dominant fusion–evaporation reaction products. Two other experiments with ^{208}Pb and ^{238}U targets were performed at the Argonne NL using the more powerful Gammasphere detector array. The high data quality is illustrated by two selected gamma coincidence spectra displayed in figure 14 which show spectacularly

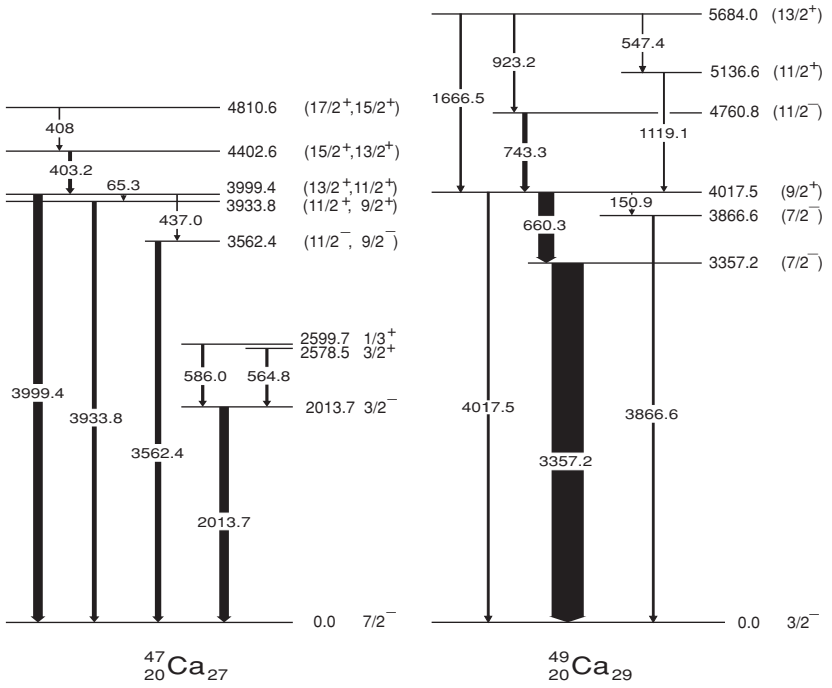

Figure 15. Yrast states in one neutron–hole ^{47}Ca and one neutron–particle ^{49}Ca isotopes established in experiments using the ^{48}Ca beam on ^{48}Ca, ^{208}Pb, ^{238}U targets [34, 35].

gamma cross-coincidences used to identify transitions in ^{49}Sc and ^{47}K. The resulting level schemes of the closest one-particle and one-hole neighbours of ^{48}Ca are shown respectively in figures 15 and 16. Whereas the extensive discussion of identified structures is presented in [34, 35]; for the purpose of this review it is worthwhile to outline the most important progress achieved in this study. In the ^{48}Ca doubly magic core nucleus the earlier information on simple particle–hole excitations was significantly solidified and the hitherto unknown new structures of high energy two-particle two-hole yrast excitations were established. In the one-particle/hole closest neighbours, ^{47,49}Ca, ^{49}Sc and ^{47}K, essentially most of the observed structures are new and correspond to the coupling of the valence particle/hole with various core excitations. Here the neutron-core excitations are reasonably well controlled in the shell model calculations, but yrast states arising in proton-core excitations, abundantly observed in experiment, still await a more educated theoretical approach possibly guided by the obtained new experimental information.

Much better and more complete quantitative results of shell model calculations are available for nuclei with $Z > 20$ and this provides substantial support for complex structures established in neutron-rich isotopes of Ti from the analyses of the same data accumulated in the above-described experiments. The identification of the first 2^+ state in the ^{54}Ti isotope [36] gave a strong reinforcement for the existence of the $N = 32$ subshell closure arising from the large energy separation of the neutron $p_{3/2}$ and $f_{5/2}$ orbitals. On the other hand the combination of highly selective radioactive decay studies of exotically neutron-rich fragmentation products performed at the MSU [37], with the deep-inelastic spectroscopic data allowed us to identify states in the ^{56}Ti isotope [38] with the low lying 2^+ state which excluded the $N = 34$ subshell closure anticipated by theoretical calculations [39]. In the region of neutron excess close to the

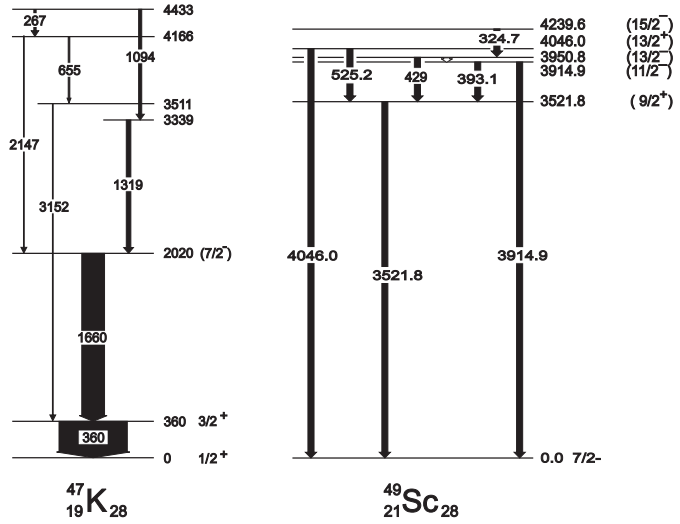

Figure 16. Yrast states of one proton–hole ^{47}K and one proton–particle ^{49}Sc nuclei established in experiments using the ^{48}Ca beam on ^{48}Ca, ^{208}Pb, ^{238}U targets [34, 35].

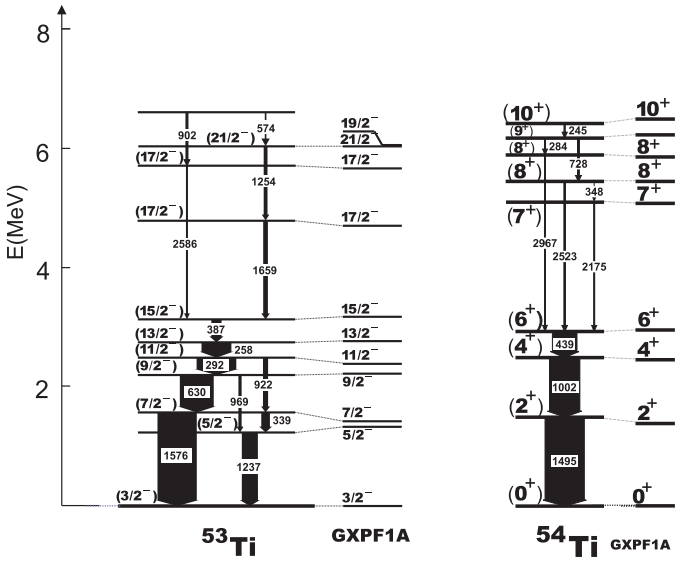

Figure 17. Level schemes of ^{53}Ti [40] and ^{54}Ti [36] isotopes established in experiments using the ^{48}Ca beam on ^{208}Pb and ^{238}U targets. Shell model calculated levels are shown to the right.

limit of DIHIR spectroscopy the radioactive decay data are very useful to identify lowest states in new isotopes, or to solidify identifications made by the cross-coincidence analysis. With this safe starting point the DIHIR data usually provide fairly complete structures involving higher lying states and extending often to high-spin values. Such structures observed, e.g., in ^{53}Ti [40] and ^{54}Ti [36] isotopes and shown in figure 17 demonstrate the potential of the technique. At the same time the observed excellent agreement with shell model calculations involving

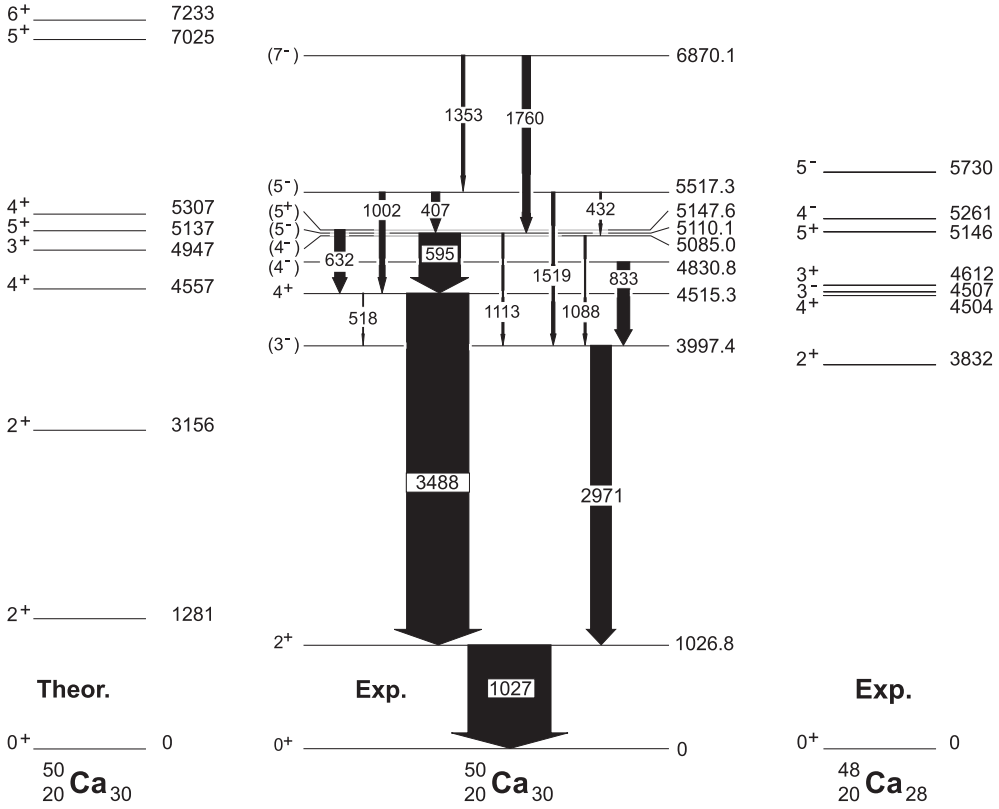

Figure 18. Yrast and near-yrast states of ^{50}Ca established in ^{48}Ca + ^{208}Pb, ^{238}U experiments. Shell model calculations involving only neutron-core excitations are shown to the left. The experimental ^{48}Ca core excitations also including proton excitations (negative parity states) are shown to the right [41].

well-established interactions of valence particles invites further extension of experimental and theoretical efforts.

The neutron-rich Ca isotopes, with the closed proton shell, are naturally the most important nuclei to follow the variation of nuclear structure with neutron excess, e.g. the $N = 32$ subshell closure is best demonstrated by the high energy of the 2^+ state in the ^{52}Ca isotope [26]. However, often the short lifetimes of states strongly limit the usefulness of the DIHIR spectroscopy in thick target experiments, unless the feeding from higher lying states provides time delay in the picosecond range. Therefore at present the heaviest Ca isotope which could be studied in this way is ^{50}Ca, for which the observed structure of levels [41] is shown in figure 18. The observed large energy gap between the 2^+ and the 4^+ states also confirms the large energy separation of the $f_{5/2}$ neutron orbital. From the same data the most important states of the other $N = 30$ isotone—^{51}Sc—could also be established [41]. In both cases the observed states can be qualitatively understood; however, at present only those involving neutron-core excitations can be safely calculated within the shell model. The current analysis of gamma angular distributions and gamma–gamma correlations will provide spin-parity assignments for most intensely populated states and this experimental input may enhance theoretical efforts to understand complete structures in a more quantitative way.

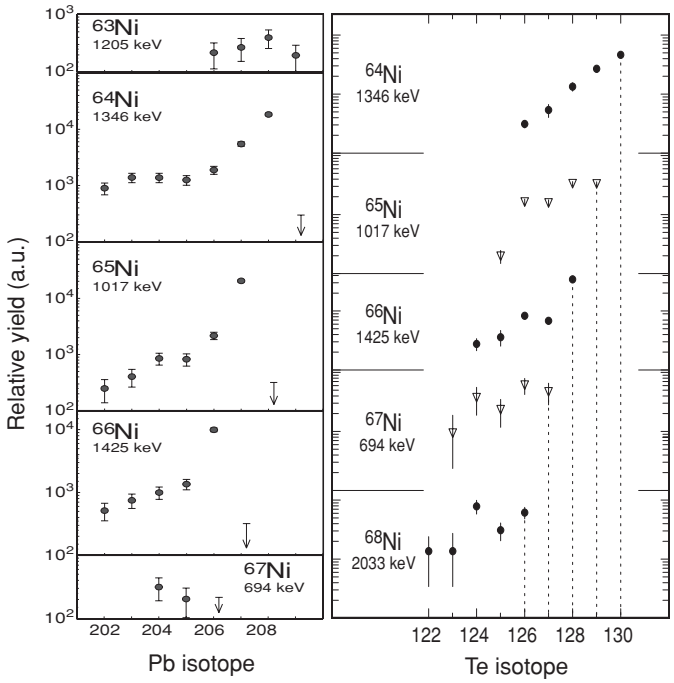

Figure 19. The identification of Ni isotopes by observed gamma cross-coincidence yields of Pb (left) and Te (right) isotopes from experiments using a ^{64}Ni beam on ^{208}Pb [42] and ^{130}Te [43] targets. For each Ni isotope the main gated gamma transition is marked. Reprinted in part with permission from [43] © 1995 American Physical Society.

4.2. Neutron-rich Ni isotopes—region around the $N = 40$ subshell closure

Beams of ^{64}Ni ions, the most neutron-rich of stable Ni isotopes, were used in several gamma coincidence experiments. In the first one performed with the OSIRIS 12 detector array at the Hahn–Meitner Institute a thick ^{208}Pb target was used and the main goal was to identify unknown yrast states in nuclei from the doubly magic ^{208}Pb region. However, the data analysis was also focused on the beam-like product spectroscopy and revealed a wealth of information on hitherto unknown yrast and near-yrast states of neutron-rich Ni isotopes. In these analyses detailed level schemes of four Ni isotopes ranging from $A = 64$ to 67 could be established [42] involving the identification of several isomeric states. Shell model calculations reproduced reasonably well experimental levels and validated tentative spin-parity assignments which were suggested by the observed gamma decays. Selected results indicating gamma cross-coincidence identifications of Ni isotopes are displayed in figure 19 and examples of level schemes are shown in figure 20.

These encouraging results enhanced attempts to identify the ^{68}Ni isotope for which some irregularity at the $N = 40$ closed neutron subshell was anticipated. Clarification of this point was considered to be a necessary step towards experimental and theoretical studies of more neutron-rich Ni isotopes. The tentative identification of the 2033 keV high energy first 2^+ excitation in ^{68}Ni suggested by the HMI experiment data was fully confirmed in a subsequent experiment performed at the INFN LNL Legnaro with the GASP array and the ^{64}Ni beam on ^{130}Te target [43] (see figure 19). The systematic of lowest spin levels in Ni isotopes is shown in figure 21. The finding of the long-lived 5^- isomer and the high energy of the first 2^+ state in the ^{68}Ni isotope invoked a clear analogy with the doubly closed $Z = 40$ ^{90}Zr isotope and

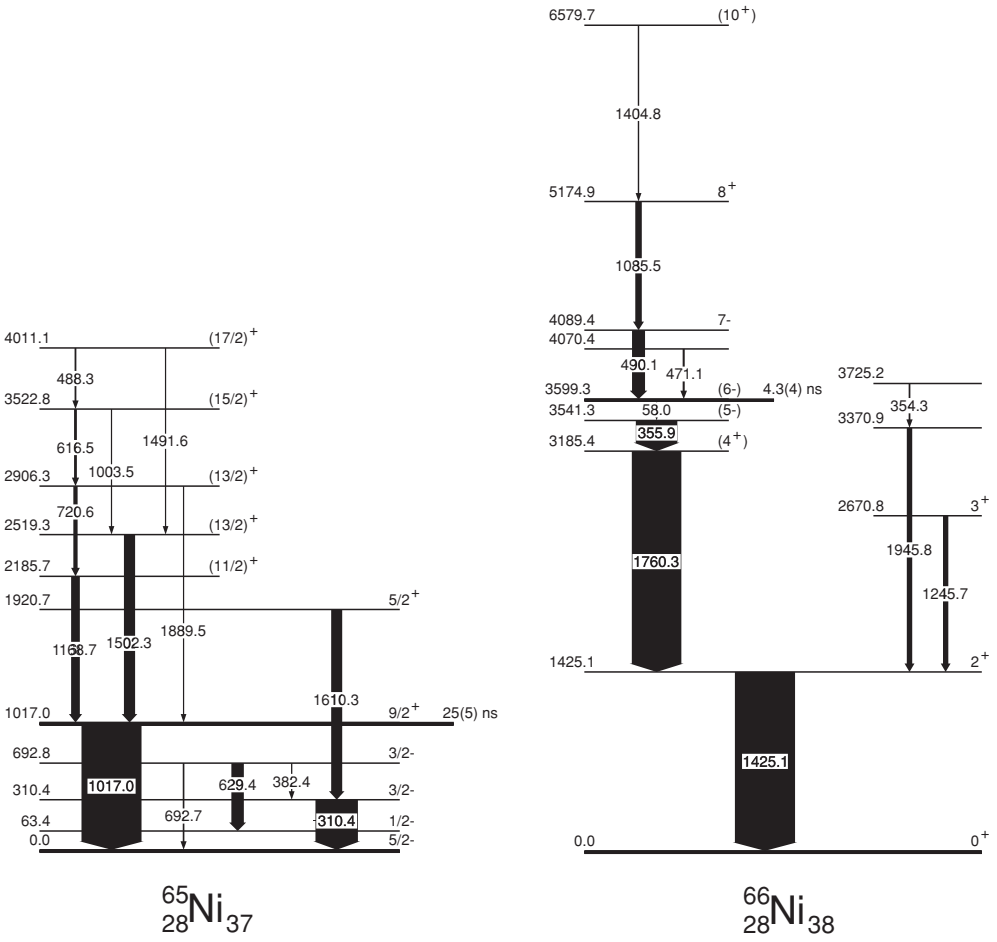

Figure 20. Level schemes of ^{65}Ni and ^{66}Ni isotopes established in ^{64}Ni + ^{208}Pb experiment [42].

suggested the $N = 40$ subshell closure, which should also manifest itself in the structure of neighbouring nuclei.

The most natural experimental continuation of this study was the search for the ^{69}Ni and ^{70}Ni isotopes, specifically directed by the straightforward expectation of the presence of the 8^+ isomeric state in ^{70}Ni. However, the fast decrease of the isotope production yield with the number of neutrons transferred to the ^{64}Ni projectile was rather discouraging. Therefore the ^{76}Ge beam was selected with a hope that proton removal from the projectile would populate a more neutron-rich range of Ni isotopes. The test experiment which used the ^{76}Ge + ^{208}Pb colliding system has shown the expected trend as displayed in figure 22, but the identification of exotic neutron-rich isotopes by the cross-coincidence technique demanded much higher statistics. In the meantime excellent experiments performed at GANIL and GSI [44] and dedicated to the search for isomeric states in neutron-rich products of the ^{76}Ge and ^{86}Kr fragmentation processes identified unambiguously many isomers including the 8^+ isomer in ^{70}Ni. This allowed us to find easily the presence of the ^{70}Ni isomer in the above-mentioned test run which confirmed the correctness of the intuitively selected way to move towards larger neutron excess. At the same time it demonstrated the superiority of techniques using the very

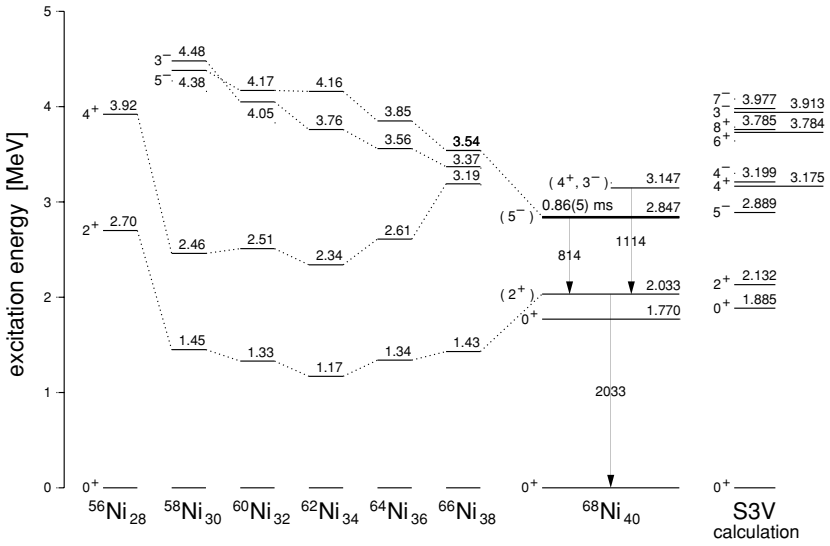

Figure 21. Systematic of lowest excited states in Ni isotopes demonstrating irregularity observed for the $N = 40$ ^{68}Ni isotope. For ^{68}Ni the shell model calculated levels are shown to the right.

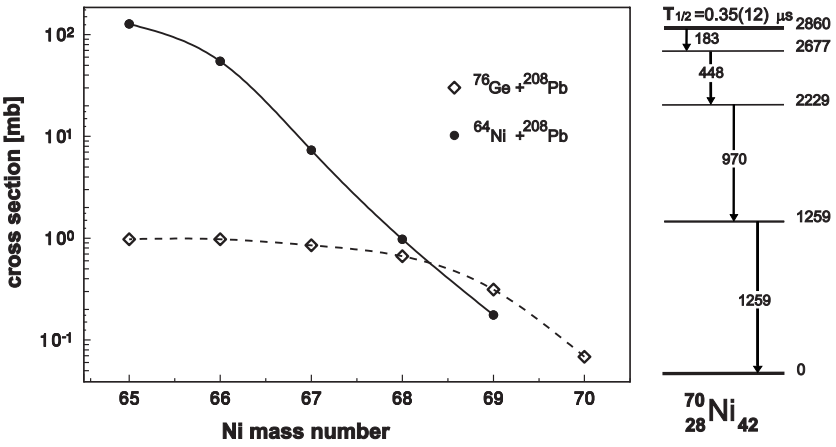

Figure 22. Production yields of Ni isotopes observed in ^{64}Ni + ^{208}Pb and ^{76}Ge + ^{208}Pb experiments aiming to identify the 8^+ isomer in ^{70}Ni isotope.

selective detection and projectile fragmentation process to identify isomeric states in very neutron-rich nuclei.

The power of the in-beam deep-inelastic spectroscopy could be better exploited in the region located closer to the stability line. Here the data analysis produced significant broadening of information on neutron-rich Fe and Zn [45] isotopes, which was even extended in parallel experiments using the Gammasphere array at the ANL Argonne [46].

Interesting results were obtained in the study of the ^{69}Cu isotope [47], which displayed structures arising from the one proton–particle coupled to the ^{68}Ni core nucleus excitations. In ^{69}Cu the long-lived isomer was identified and in conjunction with the ^{69}Ni beta decay results [48] the observed states could be easily understood within the framework of the shell

model. In parallel work by Ishii *et al* [49] a much more sensitive way of detecting isomeric states in nuclei produced in deep-inelastic collisions was applied. Thin targets were used and reaction products were stopped in Si telescope detectors, which allowed us to identify the nuclear products and to observe isomeric decays in an environment free of prompt gamma rays. This technique allowed us to identify new higher lying isomers in ^{68}Ni and ^{69}Cu [49] and states populated in their decay which could be quantitatively reproduced in simple shell model calculations using experimental two-body interactions.

Efforts to investigate neutron-rich nuclei in the ^{68}Ni region and beyond are continued and also include other odd-proton as well as odd–odd isotopes. Whereas the deep-inelastic heavy-ion reactions are used for the more detailed study of nuclei closer to the beta stability valley and also involve the detection of prompt gamma rays, the more exotic species with much larger neutron excess are studied using projectile fragmentation processes. Here the investigation is limited to isomeric states which survive the flight time determined by conditions at a specific fragment separator, yet many of the obtained results prepare the ground for future spectroscopic study when some of these exotic isotopes will be accessible in deep-inelastic reactions using radioactive beams.

4.3. Hard-to-reach Sn and Te isotopes and the five-proton ^{137}Cs nucleus

The motivation to study the neutron-rich Sn isotopes was outlined in section 2, where the identification of the 10^+ isomers in ^{122}Sn and ^{124}Sn isotopes [15] was presented as the first application of deep-inelastic heavy-ion reactions for gamma spectroscopy of nuclei inaccessible in fusion–evaporation reaction. This result initiated a much broader programme aiming to establish the seniority of $\upsilon = 2$ and 3 $(\nu h_{11/2})^n$ isomers in the whole series of neutron-rich Sn isotopes connecting at the other end the ^{128}Sn and ^{130}Sn 10^+ isomers known from the spontaneous fission product study. Already from these early experiments, in which the ^{124}Sn target was bombarded with ^{76}Ge and ^{80}Se projectiles, also the $(\nu h^2_{11/2}\ s_{1/2})19/2^+$ isomers were identified in the odd-mass ^{119,121,123}Sn isotopes [50] as a key step towards the subsequent location of higher lying yrast states. In fact, from the same data also the $(\nu h_{11/2})^n\ 27/2^-$ isomers could be identified in ^{119}Sn and ^{121}Sn isotopes [51, 52].

In order to enter more favourably the region of neutron-rich Sn isotopes the higher N/Z projectiles ^{136}Xe and ^{238}U were used to bombard the ^{124}Sn target in subsequent experiments. The observed production yields of isomeric states in Sn isotopes are shown in figure 23 and illustrate the observed shift towards more neutron-rich isotopes when ^{136}Xe and ^{238}U projectiles are used. In the ^{136}Xe experiment, a detailed level scheme of ^{123}Sn was established [51, 52] with the long-lived 34 μs $27/2^-$ isomer which reflects the half-filling of the $h_{11/2}$ subshell at the neutron number $N = 73$. Subsequently the ^{238}U run provided the identification of the corresponding isomers in ^{125}Sn and ^{126}Sn isotopes [53]; isomeric gamma decays are shown in figure 24. The main result which summarizes several years of investigation of isomeric states in a series of neutron-rich Sn isotopes is presented in figure 25 which displays the systematic of B(E2) reduced transition probabilities for isomeric transitions [53]. The spectacularly smooth decrease of the B(E2) amplitudes, crossing the zero line around $N = 73$ and going to negative values above this neutron number, reflects the filling of the neutron $h_{11/2}$ subshell. It is worthwhile to mention that this phenomenon could be followed in a much broader range than that observed earlier for the proton $h_{11/2}$ subshell in the neutron-deficient $N = 82$ isotones [14].

In a somewhat different way the systematic study of neutron-rich Te isotopes was performed from the analysis of the ^{130}Te + ^{64}Ni experimental data [54]. Here predominantly the prompt events were considered and the identification of subsequent Te isotopes was checked

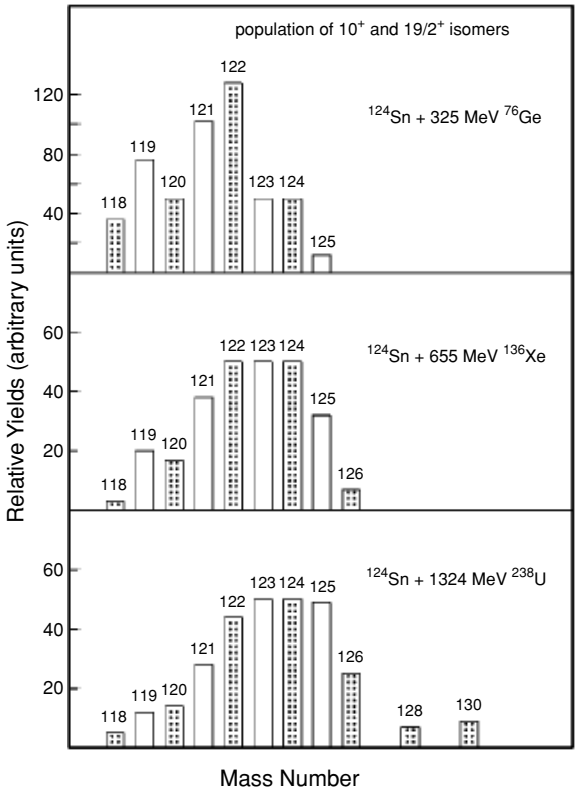

Figure 23. Production yields of Sn isotopes observed in bombardments of the ^{124}Sn target with ^{76}Ge,^{136}Xe and ^{238}U projectiles. Reprinted with permission from [53] © 2000 American Physical Society.

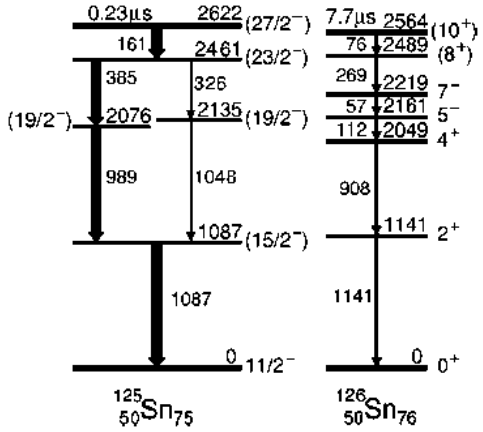

Figure 24. Decay schemes of seniority isomers established in ^{125}Sn and ^{126}Sn isotopes from the ^{238}U + ^{124}Sn experiment. Reprinted with permission from [53] © 2000 American Physical Society.

by gamma cross-coincidences with the corresponding distributions of Ni partner nuclei. The physical motivation was to study the systematic change of the nuclear structure from distinctly collective vibrational excitations in the middle of the neutron shell to single particle features

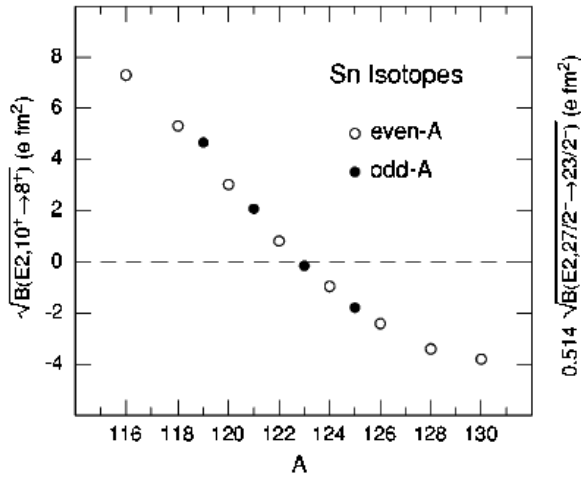

Figure 25. E2 transition amplitudes for $(h_{11/2})^n$ $10^+ \rightarrow 8^+$ and $27/2^- \rightarrow 23/2^-$ isomeric transitions in even-A and odd-A tin isotopes. The values for the odd-A nuclei are multiplied by 0.514 to compensate for different geometric factors of spin coupling. The zero line crossing determines the $N = 73$ neutron number at which the $h_{11/2}$ subshell is half-filled. Reprinted with permission from [53] © 2000 American Physical Society.

affecting the spectra for heavier isotopes on the way towards the $N = 82$ closed shell. Results included all even and odd isotopes in the $A = 126$–131 mass range [54] and also involved the identification of a number of isomeric states with clear characterization of the configuration structure. In comparison with the corresponding Sn isotopes the observed 10^+ isomers do not show a similar regularity of the B(E2) transition probabilities as they are strongly affected by the polarizing effect of two extra protons present in Te. The level scheme of ^{130}Te was recently completed [55] by the identification of the higher lying four-particle 15^- isomer. Its gamma decay helped us to locate firmly the long-lived 10^+ isomer lying only 19 keV above the 8^+ state as shown in figure 26.

In this mass region approaching the ^{132}Sn doubly magic core nucleus it is worthwhile to distinguish a specific case of the ^{137}Cs isotope studied in the ^{136}Xe + ^{232}Th reaction [56]. For many years yrast states of the $N = 82$ isotones have been studied in a broad range of proton numbers from the $Z = 50$ doubly magic ^{132}Sn to the very neutron-deficient $Z = 72$ ^{154}Hf [14]. At the neutron-rich end very complete level schemes of ^{134}Te, ^{135}I [7] and ^{136}Xe [57], correspondingly two-, three- and four-valence proton isotones, could be established from the fission spectroscopic studies. On the theoretical side the full set of diagonal and non-diagonal nucleon–nucleon interaction matrix elements could be extracted by fitting all available experimental information and provided also a precise quantitative prediction for unknown yrast levels in the ^{137}Cs five-proton isotope [58]. This, hard-to-access for the yrast spectroscopy ^{137}Cs, was the only $N = 82$ isotone which remained experimentally unknown; therefore the application of deep-inelastic spectroscopy required an unambiguous identification of lowest yrast transitions. With this aim the selection of deep-inelastic one-proton transfer in the ^{136}Xe + ^{232}Th collisions demanded the observation of the easily fissionable ^{231}Ac reaction partner nucleus with the largely unknown gamma transitions. In spite of these difficulties such identification could be achieved. The coincidence spectra displayed in figure 27 clearly show the presence of the Ac x-rays in the double-coincidence gate set on two gamma transitions which were the best candidates for ^{137}Cs as marked in the figure. Also based on other important arguments they were firmly assigned to this isotope and allowed us

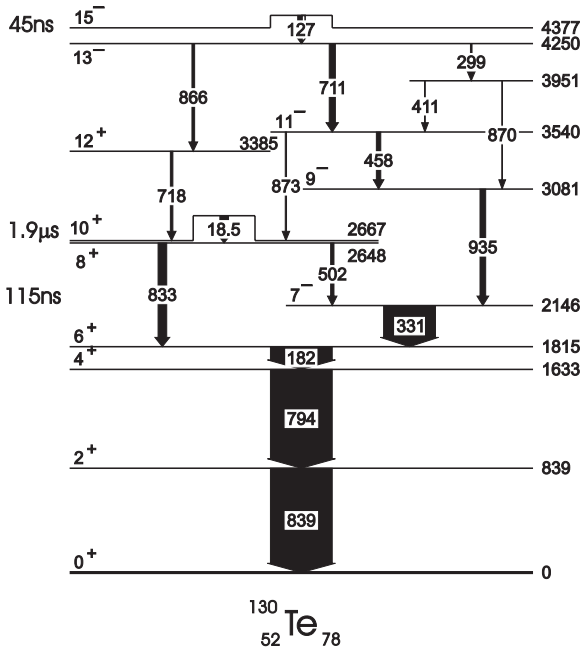

Figure 26. Gamma decay of the 15^- isomeric state in ^{130}Te established in ^{136}Xe + ^{232}Th experiment. The observed branching settles the earlier unknown energy of the lower lying 10^+ isomer [55].

to construct the ^{137}Cs level scheme shown in figure 28 which reproduced with great accuracy the structure of levels predicted in calculations. The quantitative agreement marked by small energy differences between the experimental and calculated levels illustrates spectacularly the predictive power of the phenomenological shell model approach. In the later analysis also the tentative assignment of two extended transition bands could be made in the ^{231}Ac reaction partner nucleus.

4.4. New K-isomers

It was very early realized that in the final nuclei produced in deep-inelastic heavy-ion reactions population of states is not selective to their structural properties. Similarly as in the fusion reaction products the spin and energy distribution of populated states appears to be governed only by the reaction dynamics which for binary reactions defines in a more complex way the range of angular momentum and energy transfer. Therefore it was not surprising that in collisions of ^{64}Ni with ^{208}Pb, where some deep-inelastic reaction products fall in the range of deformed nuclei characterized by systematic occurrence of the K-isomerism, one could easily observe the copious population of such isomers [18, 20] known from previous studies. Following the early experimental observations [59] the phenomenon of K-isomers [60] was theoretically predicted [61] to occur abundantly in the $A \sim 180$ mass region nuclei and many such isomers were identified using fusion–evaporation reactions. The range of nuclei which could be accessed in fusion reaction using the available stable isotopes for targets and projectiles restricted this investigation to the neutron-deficient side of the valley of stability and resulted in a large gap in the experimental information on high-K isomers in neutron-rich isotopes. As a consequence, theoretical predictions of very high-spin yrast isomers in the $A \sim 180$ region [61] remained untested for more than two decades.

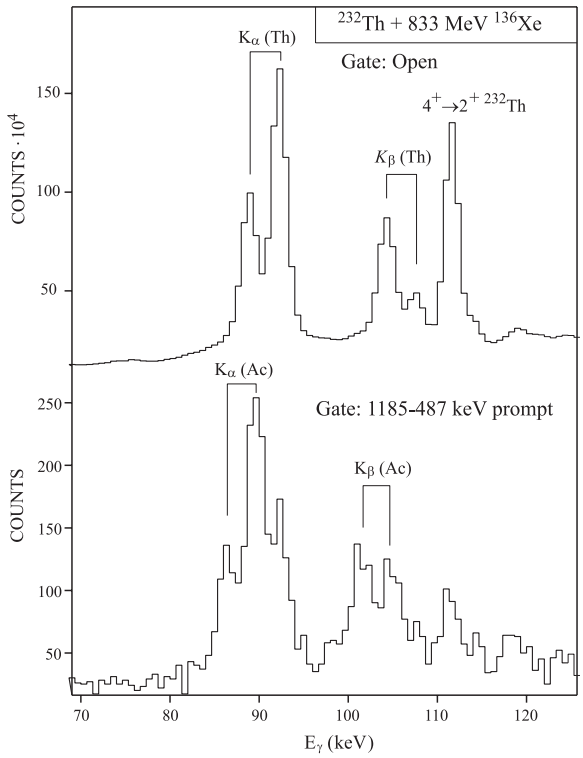

Figure 27. Low energy parts of gamma coincidence spectra settling the identification of yrast transitions in ^{137}Cs produced in one-proton transfer in ^{136}Xe + ^{232}Th collisions. The projection spectrum (upper) is dominated by the presence of Th target x-rays and double gate set on ^{137}Cs transitions (lower) strongly selects x-rays from the Ac reaction partner. Reprinted with permission from [56] © 1999 American Physical Society.

It was obvious that using beams of neutron-rich nuclei to bombard targets of available neutron-rich isotopes in the $A \sim 180$ region will allow us to identify many new isomers in nuclei produced in deep-inelastic reactions. A successful attempt was made by Wheldon *et al* [62] with the pulsed ^{238}U beam and series of targets of the heaviest stable isotopes of ytterbium, lutetium, tantalum and tungsten. Along with the observation of many well-known isomers in nuclei produced in multi-particle transfer reactions the experiment provided the identification of five strongly populated new isomeric states in the target nuclei. One should note that the production of high-spin excitations in the target nucleus involves many complex processes from deep-inelastic nuclear excitation to few nucleon transfer reactions followed by subsequent evaporation of the same number of nucleons and the integrated production yield is usually comfortably large. The five new isomers could therefore be fully characterized, their lifetimes allowed us to extract hindrance factors, and excitation energies could be compared to theoretical calculations which indicated the configuration assignments and transparent structural interpretation. From the same experiment the K-isomer in ^{185}Ta could be identified [63] and the impressive harvest of new isomer identifications was obtained from the subsequent Gammasphere experiment in which the neutron-rich ^{180}Hf was bombarded with ^{238}U beam [64–66]. This line of study was then successfully continued using the ^{208}Pb fragmentation process which entered an even more neutron-rich region of nuclei [67, 68]. With the perfect A and Z identifications of fragmentation products the sensitivity of such a technique allows

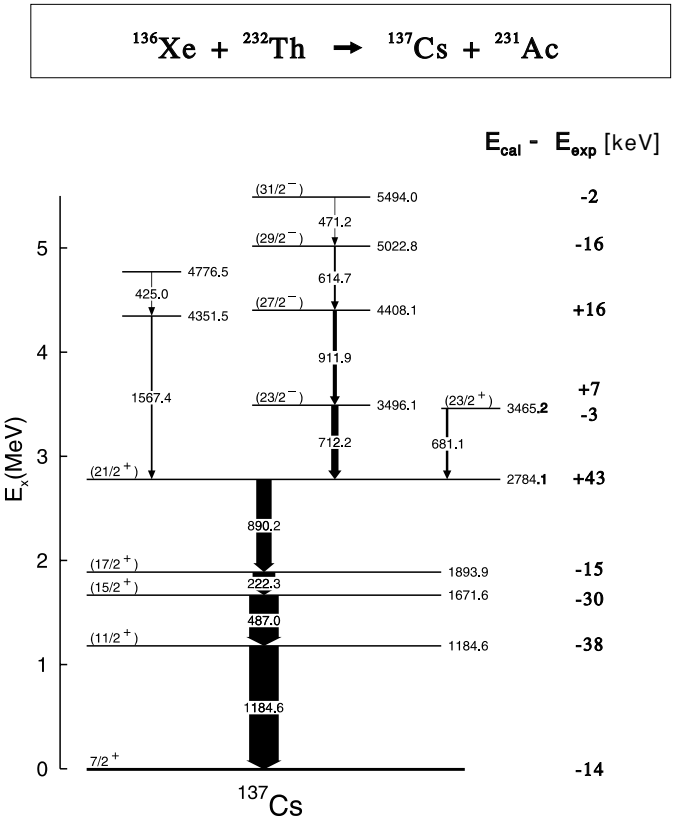

Figure 28. Yrast levels in the ^{137}Cs isotope established from ^{136}Xe + ^{232}Th experiment [56]. The indicated energy differences of calculated (prior to experiment) and experimental levels illustrate the predictive power of shell model calculations using experimental two-body matrix elements.

us to observe very exotic species produced with low cross sections. However, the detection is restricted to isomeric states only and therefore the transition ordering in the isomeric decay is sometimes difficult.

4.5. Nuclei in the doubly magic ^{208}Pb region

The application of deep-inelastic reaction spectroscopy to study yrast states in nuclei from the doubly magic ^{208}Pb region turned out to be most productive. Opening the previously very much restricted area of high-spin excitations in these shell model nuclei resulted in a significant broadening of experimental information; e.g. states with record spin values above $I = 26$ were populated in the specific case of the doubly magic ^{208}Pb core nucleus. In fact the gradual progress in revealing high-spin state structures of the ^{208}Pb core nucleus marks probably in the best way the growing potential of deep-inelastic reaction techniques with increasing availability of heavy-ion beams and the improving detection sensitivity of large gamma detector arrays.

Prior to the first experiments aimed at studying the ^{208}Pb in ^{64}Ni + ^{208}Pb collisions [69], only a few important high-spin states could be located in the (e, e′) and (p, p′) [70] scattering experiments up to the 14^- highest spin state arising from the simple neutron particle–hole

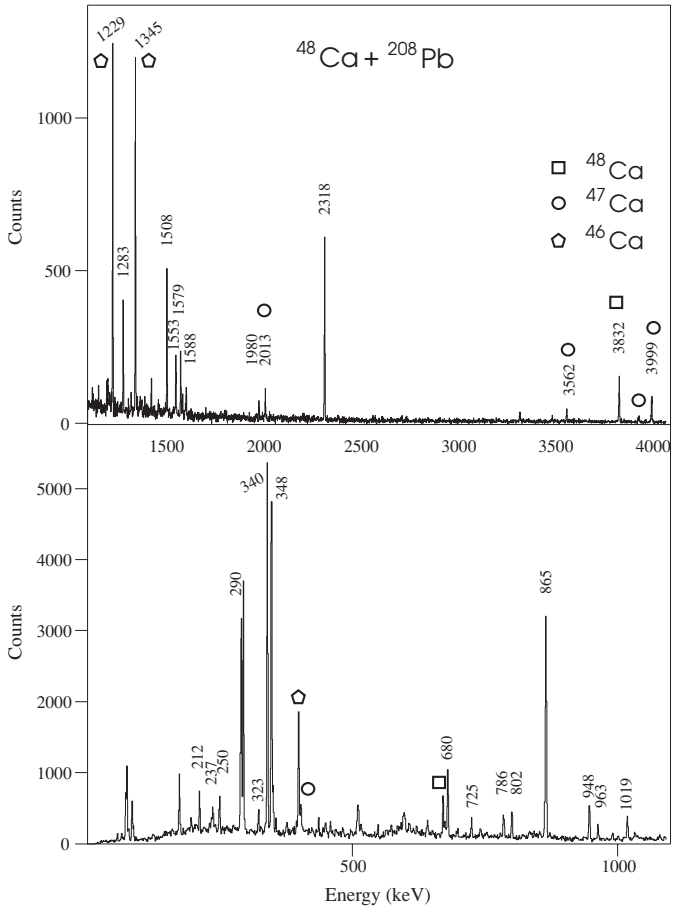

Figure 29. Gamma double-coincidence projection for transitions preceding the 10^+ isomer in ^{208}Pb from ^{48}Ca + ^{208}Pb experiment. Events were selected by gating the delayed, most intense transitions occurring in the isomeric decay. Apart from cross-coincidence transitions from Ca isotopes marked in the spectrum, all other lines correspond to higher lying transitions in the ^{208}Pb nucleus [55].

excitation. For the first time the gamma decay of these known states and a few other ones could be easily observed and characterized already from the first deep-inelastic reaction gamma coincidence data [69]. Subsequent experiments using ^{76}Ge, ^{136}Xe and ^{208}Pb beams on the thick ^{208}Pb target provided a more detailed level scheme including higher spin states and tentatively located high-spin isomers [71, 72]. However, the full scale analysis performed with excellent data obtained at the Argonne NL in the experiment using the high energy ^{48}Ca beam on a thick ^{208}Pb target and the powerful Gammasphere detector array provided the most significant progress [35, 55]. The clean selection of events arising from the high-spin excitations of ^{208}Pb was achieved by using delayed coincidences with gamma transitions below the 500 ns 10^+ isomer. The double-gamma coincidence projection obtained with this selection is shown in figure 29 and the complex level scheme obtained from the analysis is displayed in figure 30. Although the final spin-parity assignments still await the outcome of the detailed analysis of the angular correlation data, the tentative characterizations based on the observed gamma decay and general yrast arguments can be compared to a sequence of yrast levels

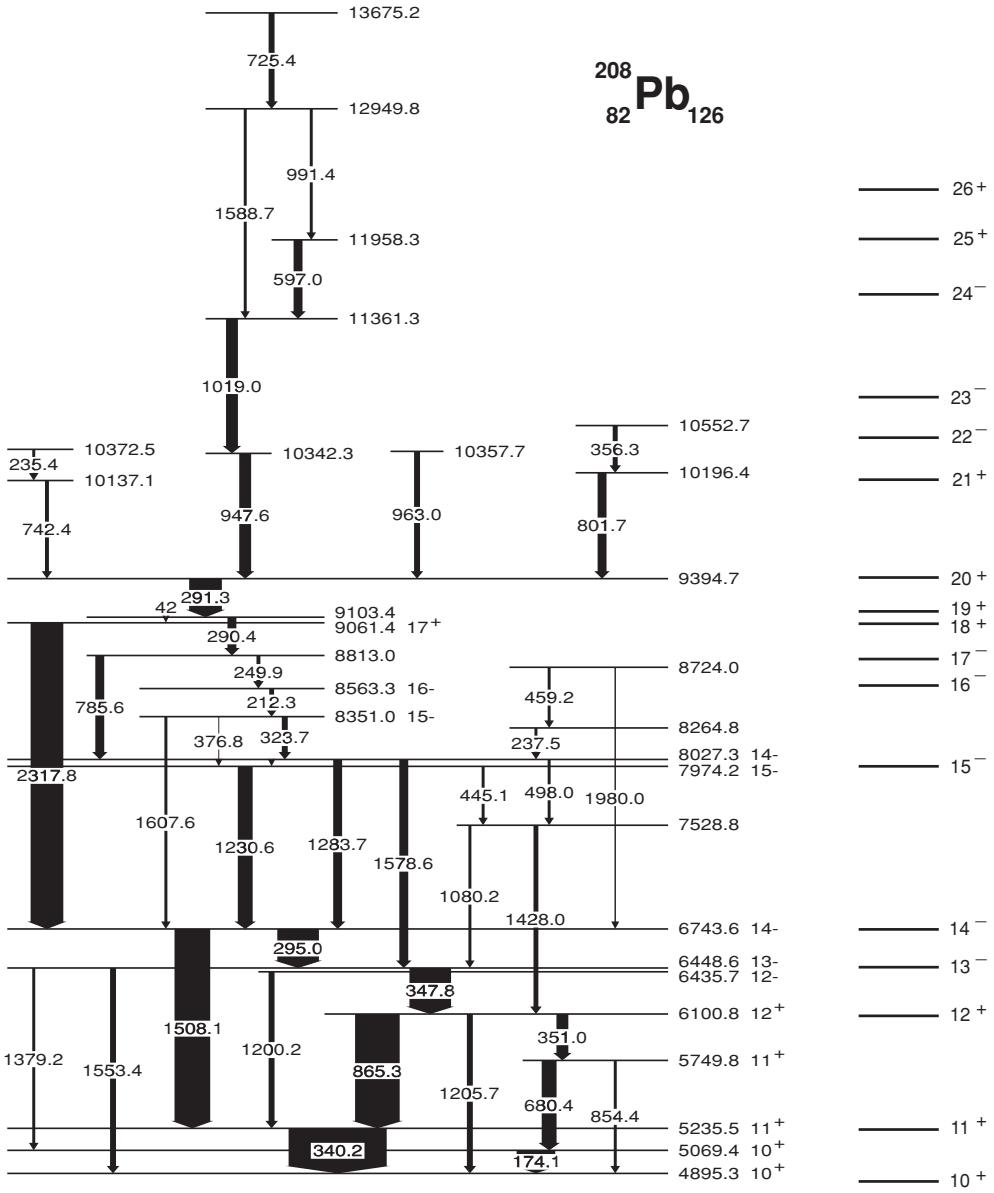

Figure 30. High-spin states above the 10^+ isomer in ^{208}Pb established mainly from the ^{48}Ca + ^{208}Pb experiment [55]. Selected yrast levels calculated within the shell model using the best available two-body matrix elements are shown to the right.

calculated from the shell model which employed the best set of available two-body interactions. It is apparent that the observed states reach spin values above the $I = 26$ calculated level and the highest lying states must involve complex four-particle four-hole structures.

From the same sequence of experiments the high-spin states of the ^{207}Pb isotope were studied starting with the identification of the strong 2486 keV transition located immediately above the $i_{13/2}$ neutron–hole long-lived isomeric state [73]. This transition, wrongly assigned earlier as the double-octupole phonon in ^{208}Pb [74], represents in fact the octupole vibration

of the ^{208}Pb core coupled with the $i_{13/2}$ neutron–hole. Its distinct yrast location ensures that nearly all higher spin population intensities proceed in the decay via this state, which simplified the identification of many higher lying states. The tentative identification of the high-spin long-lived isomeric state in ^{207}Pb was reported several years ago [71], but new experimental data revealed much more detailed information. The final analysis of those Gammasphere experiments was only recently completed and the publication of results showing the complex level scheme of ^{207}Pb, up to similarly high-spin values as in the ^{208}Pb isotope case, is in the preparation stage [75]. It can now be mentioned that the shell model calculation reproduces with surprisingly good accuracy most of the observed levels and this will be discussed in a forthcoming publication.

Already the early analyses were focused on the more neutron-rich Pb isotopes and transparent high-spin state structures were established in the ^{209}Pb [76] and ^{210}Pb [77] isotopes. Recently also the most important yrast states arising from the three-neutron configurations in the largely unknown ^{211}Pb isotope could be identified [78]. Here the number of experiments helped us to provide an unambiguous identification, but the essential spectroscopic information came from the analysis of the ^{208}Pb + ^{238}U experimental data. The sequence of yrast transitions established the level scheme up to the 5.6 MeV energy which includes three isomeric states with distinct three-neutron configurations.

Generally the whole set of coincidence data collected in a number of experiments contains events from many nuclei in the shell model region around the doubly magic ^{208}Pb core and until now the analysis was focused only on selected cases of interest where the previous experimental information was very incomplete. In this way the detailed analysis of the important proton neutron–hole nucleus ^{208}Bi yielded an extended scheme of excitations [79] of the transparent shell model structure at high-spin states. Also the previously inaccessible new high-spin levels and isomeric states could be established in the ^{211}Bi [80] and ^{211}Po [81] nuclei providing guidance to the further improvement of the quantitative shell model approach in the region.

The neutron-rich nuclei below ^{208}Pb, the one proton–hole Tl and two proton–hole Hg isotopes are particularly attractive objects for spectroscopic analysis since here the earlier experimental access was very much restricted. Efforts to obtain essential initial identifications for Tl and Hg isotopes with neutron number above the $Z = 126$ line have not yet provided satisfactory results, but new high-spin state structures could be observed in several less exotic, e.g. ^{206}Tl and ^{207}Tl, isotopes [82]. Also the extended high-spin state structure above the earlier known low-lying isomeric states of ^{205}Tl was recently reported [83]. It included the identification of the new $35/2^-$ isomer arising from the coupling of the $h_{11/2}$ proton–hole with two $i_{13/2}$ neutron holes and located rather transparent yrast structure above it with a predominantly populated octupole vibrational state.

One of the most important results was the identification of the high-spin state structure in the two proton–hole nucleus ^{206}Hg [84]. Several earlier attempts to locate the expected 10^+ isomer arising from the two $h_{11/2}$ proton holes were not successful, since for the used colliding systems the ^{206}Hg production yield was too small to observe any states above the known 5^- 2.1 μs isomer. Suitable production yield was obtained in the experiment using the Gammasphere and the ^{208}Pb + ^{238}U collisions with beam pulsing allowing us to observe clean delayed coincidences across the long-lived isomer as shown in figure 31. The 10^+ isomer was readily identified and the measured half-life yielded the isomeric transition B(E2) reduced probability which defined the important value of the 1.60(7)e effective charge for the $h_{11/2}$ proton hole. The obtained level scheme is shown in figure 32 and it includes transparent interpretation by indicating shell model configurations attributed to each of the observed states.

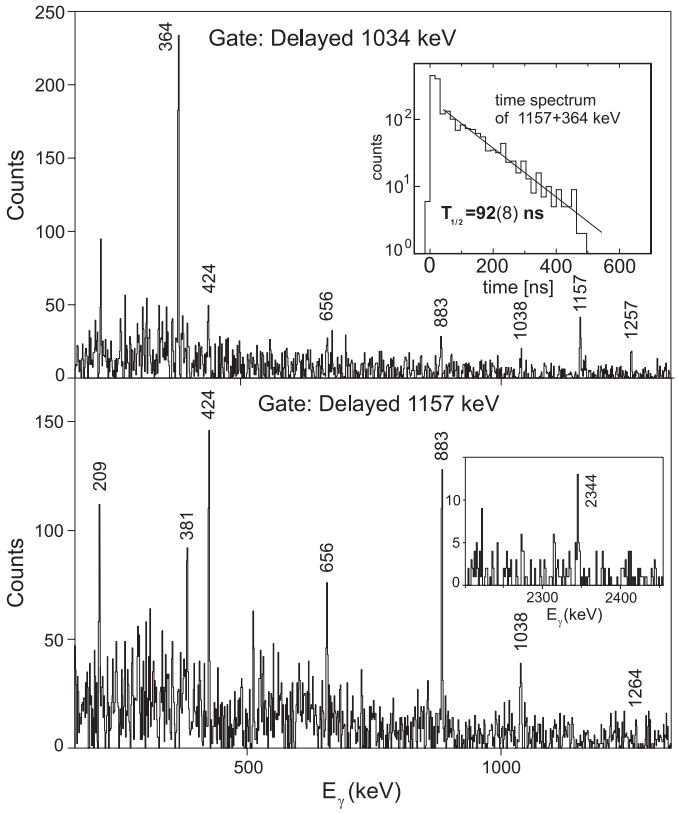

Figure 31. Gamma coincidence spectra gated by appropriate delayed transitions to identify transitions located above the 5^- (upper) and 10^+ (lower) isomers in ^{206}Hg. Reprinted with permission from [84] © 2001 American Physical Society.

An interesting physical phenomenon which could be observed in deep-inelastic reaction spectroscopic studies of the ^{208}Pb region is related to the octupole vibration of the core which is the lowest excited state in ^{208}Pb and practically the only collective mode present in yrast structures of most nuclei in the region. In many of the studied nuclei the states arising from the maximum spin coupling of the available valence particles and/or holes are usually isomeric and mark the spin and energy range where the ^{208}Pb core excitations must enter to built structures above it. The 3^- octupole vibration is naturally the first energy-favoured excitation and its stretched coupling with the corresponding multiparticle state gives rise to the yrast state usually strongly populated in the yrast cascade from higher lying states. Figure 33 displays the high energy part of the total gamma coincidence projections from experiments using the ^{208}Pb (a) and ^{136}Xe (b) beams on the ^{208}Pb target. Most of the lines seen in these spectra could be identified as transitions depopulating such octupole vibration states built on the simple shell model high-spin states in various nuclei of the ^{208}Pb region. The large collection of such transitions allowed us to systematize the observed energy shifts of coupled octupole phonon states with respect to the unperturbed energy of the 2.615 MeV 3^- phonon in the ^{208}Pb core nucleus [55, 85]. It turned out that simple addition of energy shifts observed for the octupole phonon coupling with the corresponding individual particle (hole) states reproduces surprisingly well energy shifts observed for more complex states. In figure 34 a few examples illustrating the validity of this additivity rule for two-particle (hole) states are displayed and

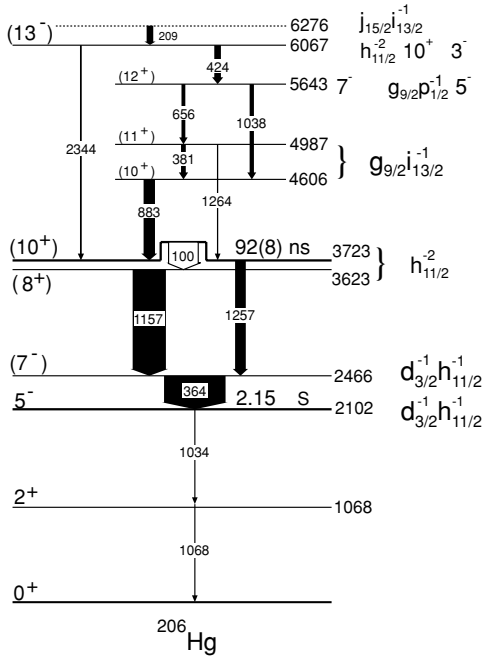

Figure 32. The ^{206}Hg level scheme established in the ^{208}Pb + ^{238}U experiment. Shell model configurations representing predominant amplitudes in state structures are indicated. Reprinted with permission from [84] © 2001 American Physical Society.

recent identification of other cases, e.g. in the three-hole ^{205}Tl isotope [83] indicates that such a rule seems to work also for more complex states.

It is rather obvious that at present the potential of deep-inelastic reaction spectroscopy in the ^{208}Pb region of nuclei is far from being exhausted and in the future yet higher spin ranges and more neutron-rich isotopes will be explored using this technique.

4.6. The heavy actinide nuclei

The thick target Coulomb excitation experiments performed by Ward *et al* [86] demonstrated that one can reach high-spin excitations in actinide nuclei by discrete spectroscopy since up to the very high-spin values an integral feeding time is long enough to stop the excited products before the gamma emission takes place. High-spin states in plutonium nuclei from $A = 238$ to $A = 244$ were subsequently studied by Wiedenhover *et al* [87] using single-neutron transfer and Coulomb excitation reactions with ^{208}Pb and ^{207}Pb beams incident on various plutonium targets. It was naturally expected that in parallel experiments using deep-inelastic reactions this feature would also permit the study of high-spin excitations in heavy actinide products, provided they can sustain fission. Unfortunately the high excitation energy involved in deep-inelastic reactions results in a strong predominance of the fission process in the decay of primary heavy fragments and only a small part of the total production cross section might allow their direct spectroscopic study. This is also reflected in difficulties encountered in the gamma cross-coincidence identification of beam-like products when the heavy actinide nuclei are used as targets. The ^{238}U target having the largest available N/Z ratio is frequently used to increase the yield of neutron-rich isotopes aimed at spectroscopic investigation; however, the analysis has to be supported by knowledge of a few lowest lying transitions identified

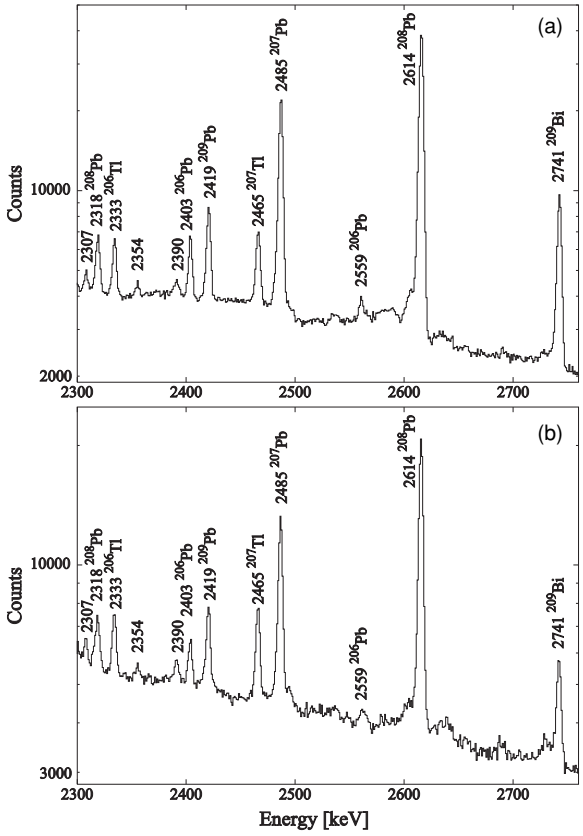

Figure 33. High energy part of gamma coincidence projection from experiments using ^{208}Pb (a) and ^{136}Xe (b) beams on ^{208}Pb target. Lines corresponding to E3 transitions identified in nuclei from the ^{208}Pb region are indicated [85].

earlier in other experiments. In spite of these difficulties the ^{238}U + ^{208}Pb experiment allowed us to observe extended new rotational bands in ^{237}U, ^{239}U and ^{240}U [80] isotopes which have shed new light on the local region of strong octupole correlations first identified around ^{239}Pu. Also the identification of the ^{231}Ac bands obtained as a byproduct in the ^{137}Cs isotope study described in section 4.3 shows the potential for using deep-inelastic reactions for the spectroscopy of actinides.

The most spectacular example of dedicated experiments to study Rn, Ra and Th isotopes in multi-nucleon transfer reactions was presented by Cocks *et al* [88, 89]. The physical motivation was clearly defined by early observation of rotational bands with alternating parity states which constitute a fingerprint for octupole deformation and reflection-asymmetric shapes of rotating nuclei [90–92]. The prediction was that the intrinsic electric dipole moments of such states will give rise to transitions with large B(E1) values connecting states of opposite parity [93]. To study this phenomenon required the observation of high-spin states in Rn, Ra and Th isotopes that are impossible to access in the fusion evaporation reaction, specifically in a very little known series of isotopes around the neutron number $N = 134$ where such an effect should manifest itself in the clearest way. The earlier successful use of deep-inelastic reactions for spectroscopy in thick target experiments offered the best chance to access these nuclei via

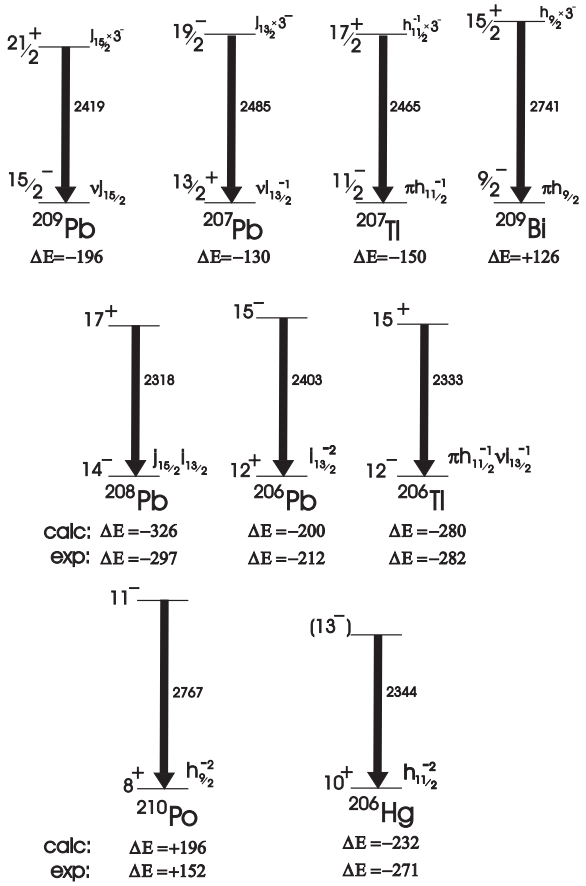

Figure 34. Examples of octupole vibration states built on high-spin states and identified in nuclei from the ^{208}Pb region. E3 transitions shown in the upper line determine energy shifts arising from the octupole vibration coupling with simple one-particle (hole) states. Energy shifts observed for those built on the two-particle (hole) states and shown below demonstrate the additivity of two structural component shifts [55, 85].

multi-nucleon transfer reactions. The ^{232}Th target was selected and the final run was preceded by test experiments using the ^{56}Fe, ^{86}Kr and ^{136}Xe beams probing the population range of heavy isotopes. From the analysis summarized in [23] it was concluded that the ^{136}Xe + ^{232}Th reaction offered the largest yield for radon and radium isotopes around $N = 134$ neutron number. This reaction was subsequently studied using the Gammasphere germanium detector array to collect γ-ray coincidence data. The quality of the data is illustrated by gamma coincidence spectra shown in figure 35 and completeness of obtained results is demonstrated by examples of band structures established in Rn isotopes displayed in figure 36. The interleaving bands with opposite parity have been observed to high spin ($I \sim 28$) in ^{218,220,222}Rn, ^{222,224,226,228}Ra and ^{228,230,234}Th isotopes. The rotational alignment properties of observed octupole bands revealed information concerning the role of the octupole phonon and the onset of stable octupole deformation with increasing rotational frequency. The magnitude of the extracted intrinsic electric dipole moments also provided additional information concerning the strength of octupole interactions in these nuclei.

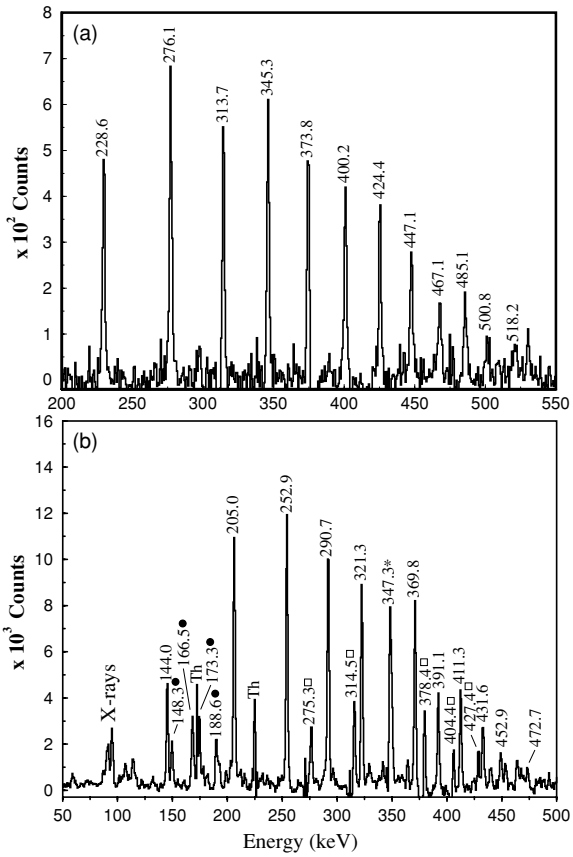

Figure 35. Gamma spectra showing transitions in ^{224}Ra (a) and ^{226}Ra (b) obtained from the ^{136}Xe + ^{232}Th experiment with corresponding double-coincidence gates. Filled circle labels mark E1 transitions and label $*$ denotes a doublet. Reprinted with permission from [89] © 1999 Elsevier.

5. Comments on thin target experiments

The present review summarizes the application of deep-inelastic heavy-ion reactions for spectroscopy of hard-to-reach nuclei in experiments using thick targets and exclusively γ-ray detection. This approach turned out to be most productive; however, much effort was devoted to techniques combining gamma-ray coincidences with direct detection of fragments produced in binary reactions. These experiments must use thin targets and the main difficulty lies in the precise determination of the velocity vector of recoiling fragments, thereby allowing us to properly correct the Doppler shift and to achieve satisfactory energy resolution in associated gamma spectra. In this procedure one has to choose the appropriate correction for the beam-like or target-like products and correspondingly gammas emitted from the other fragment contribute to the uncorrected background. Apart from this difficulty such experiments usually provide data with much lower statistics, nevertheless there are also clear advantages in applying these techniques in dedicated cases. Specifically such techniques might be very important for future spectroscopy in more exotic regions of nuclei.

Firstly, these experiments are much more selective and most often they allow us to obtain perfect isotopic identification of the detected fragment. This is particularly important for the

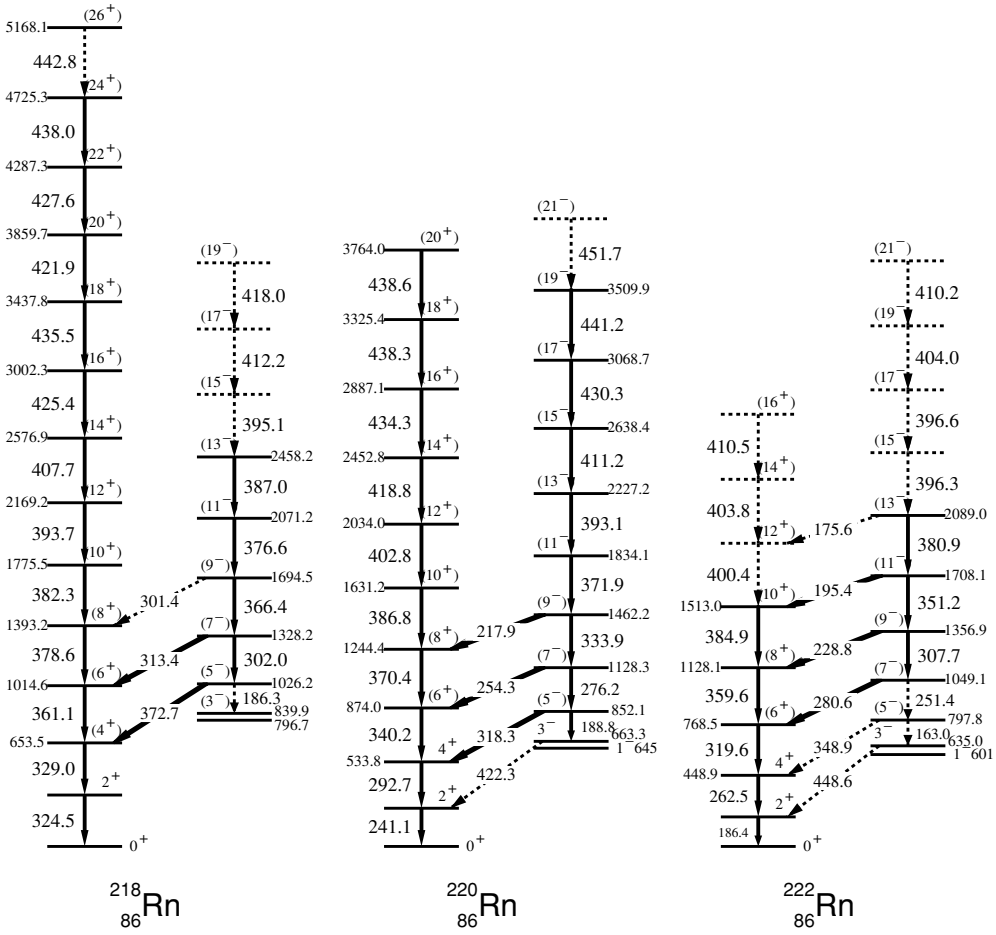

Figure 36. Level schemes of radon isotopes established from the ^{136}Xe + ^{232}Th experiment. Reprinted with permission from [89] © 1999 Elsevier.

identification of new neutron-rich nuclei that are produced with very small yields and cannot at present be recognized by the gamma cross-coincidence analysis. Secondly, short-lived states which remain undetected in thick target experiments can now be easily observed applying an appropriate Doppler shift correction. Finally, the selection of reaction kinematics allows us to control the nuclear alignment and thereby enables spin assignments by measuring correlated γ-ray angular distributions.

Various techniques and experimental details involving fragment detection in deep-inelastic reactions would require a much broader review; here we shall restrain ourselves to recalling only a few examples of these types of experiments.

Efforts to use silicon detectors for detecting heavy fragments in coincidence with gamma rays started very early and were continuously developed taking advantage of improving quality and size of both silicon and germanium detectors. Experiments demonstrating this technique were performed at the LBNL Berkeley following the encouraging observations of high gamma multiplicity in deep-inelastic reactions with rare earth beams and targets [94, 95] which prompted attempts to study high-spin states in these nuclei. Interesting examples of results

reported by Lee *et al* [96] were obtained using self-supporting 1 mg cm^{-2} targets of ^{176}Yb and ^{208}Pb bombarded with beams of ^{48}Ca and ^{154}Sm. The annular silicon strip detector was used to detect the scattered fragments covering a broad range of polar and azimuthal angles and then the available parts of the Gammasphere array were used for the gamma detection. New high-spin states were established in several neutron-rich nuclei extending to $I = 20$ spin value and in particular for the ^{175,177,178}Yb isotopes the high-spin state structures were observed for the first time. It was also concluded that the Doppler broadening limits the observation of higher spin states.

An impressive example of a dedicated instrument to detect heavy fragments of binary reactions is the CHICO detector applied successfully in spectroscopy of various binary reaction products [97]. The high resolution of this position sensitive gas-filled detector allows us to determine the direction of recoiling products with good accuracy. Initially tested in spectroscopy of the ^{252}Cf spontaneous fission products it has proven a device which significantly extends the range of observed high-spin states. The CHICO detector coupled with the large Gammasphere array provided many spectroscopic results for deep-inelastic reaction products, e.g. [98–101], as well as for the 30 MeV α-induced fission of ^{238}U [102].

A very promising tool increasing the selectivity and consequently the detection sensitivity in deep-inelastic reaction spectroscopy is the recently built large acceptance magnetic spectrometer for heavy ions. The PRISMA spectrometer [103] combined with the CLARA gamma detector array [104] is installed at the INFN Legnaro National Laboratory and has been fully operational since March 2004. The large acceptance ($\sim$80 msr and 20% $\Delta p/p$) of the PRISMA spectrometer and high $\Delta A/A$, $\Delta Z/Z$ resolution allows unambiguous fragment identification. Being correlated with the relatively high photo-peak efficiency (3%) of the CLARA gamma detector array it allows us to locate new excited states in hitherto unknown neutron-rich nuclei. Some interesting initial results have already been reported [105].

In a similar effort a variable mode high-acceptance spectrometer VAMOS was built in the GANIL laboratory to identify reaction products in experiments using the SPIRAL-accelerator beams [106]. It is coupled with the efficient EXOGAM gamma detector array and also serves to study nuclei produced in deep-inelastic reactions. Here the prospects to exploit radioactive beams for accessing exotic regions of neutron excess are particularly realistic and connected with the further development of the SPIRAL project.

6. Final remarks

The present review focused on thick target experiments exploiting deep-inelastic reactions for spectroscopy of hard-to-reach nuclei located at the neutron-rich side of the β stability valley. Results obtained in various regions of the nuclide chart document fast progress achieved in acquiring experimental information which prepares the ground for more advanced efforts aimed at elucidating the variation of the nuclear structure with the changing isospin composition of nuclear matter. Besides this line of research, the previously inaccessible yrast structures of classical shell model nuclei could be studied up to high-spin excitations thereby allowing to check the validity of the simple shell model theoretical approach in describing quantitatively complex excitations. The high-quality gamma coincidence data collected for many colliding systems are not yet completely analysed and contain many events which may potentially provide new spectroscopic information in practically all regions of the nuclide chart. Here the progress relies mainly on initial identifications obtained from other more selective experiments. The prospects for further improvement of gamma-ray detection efficiency and resolution power, which are realized within new projects of large γ-ray tracking arrays—AGATA and GRETA—might open novel lines of research also in experiments using thick

targets. Apart from the increased detection sensitivity for spectroscopy of new exotic nuclei, the deep-inelastic reaction mechanism can possibly be studied in a much more detailed way gaining deeper insight into the correlated transfer of mass, excitation energy and angular momentum.

It seems proper to consider a question: to what extent can these relatively simple experiments combined with a much more complicated data analysis can be applied in future studies with radioactive beams? The use of radioactive beams practically excludes thick target experiments due to the large background of gamma rays from the decay of collected beam nuclei. In specific cases the target thickness can be selected in a way to ensure nearly complete transmission of light radioactive beam nuclei and stopping of the desired heavy fragments. However, apart from this problem, the possibility of producing very neutron-rich nuclei with radioactive beams is still to be learned. The well-established strong tendency to equalize N/Z ratios of colliding nuclei would require both of them to be very neutron-rich in order to access exotically large neutron excess.

One has to also point out the more general shortcoming of the thick target technique which concerns spin-parity assignments for the observed states. It has been a major difficulty in completing the spectroscopic information since the full integration of reaction kinematics in thick target experiments practically reduces the average spin alignment and consequently the anisotropy of gamma radiation is very small. It turned out that the high statistics data obtained already in some experiments allow us to obtain meaningful results from the gamma angular correlation analysis and in the future this probably will be the main method to obtain necessary spin-parity assignments. In conclusion one may express safe anticipation that deep-inelastic heavy-ion reaction spectroscopy will remain for many years a powerful source of experimental information on hard-to-access nuclei.

Acknowledgments

A number of research groups contributed to the results presented in this review, and many of them collaborated closely with the Krakow spectroscopy group, which from the initial experiments has had a leading role in conducting this research. The author expresses sincere gratitude to all participants of this endeavour whose names are listed in cited publications. The author wants to address special thanks to B Fornal and other physicists of the Krakow group: J Wrzesinski, W Krolas and T Pawlat, whose expertise and involvement in this research was predominant.

Through many years the research was partly sponsored by grants of the Polish Science Committee and the present sponsoring with the grant no. 1 P03B 059 29 is warmly acknowledged.

References

[1] Nazarewicz W 1999 *Nucl. Phys.* A **654** 195c
[2] Nazarewicz W and Casten R F 2001 *Nucl. Phys.* A **682** 295c
[3] Brown B A 2001 *Prog. Part. Nucl. Phys.* **47** 517
[4] Ahmad I and Phillips W R 1995 *Rep. Prog. Phys.* **58** 1415
[5] Durell J L *et al* 1995 *Phys. Rev.* C **52** R2306
[6] Guessous A *et al* 1995 *Phys. Rev. Lett.* **75** 2280
[7] Zhang C T *et al* 1996 *Phys. Rev. Lett.* **77** 3743
[8] Fornal B *et al* 2001 *Phys. Rev.* C **63** 024322
[9] Bhattacharyya P *et al* 2001 *Phys. Rev.* C **64** 054312
[10] Broda R *et al* 1990 *Phys. Lett.* B **251** 245

[11] Broda R *et al* 1994 *Phys. Rev.* C **49** R575
[12] Bromley D A 1984 *Treatise of Heavy Ion Science* (New York: Plenum)
[13] Daly P J *et al* 1980 *Z. Phys.* A **298** 173
[14] McNeill J H *et al* 1989 *Phys. Rev. Lett.* **63** 860
[15] Broda R *et al* 1992 *Phys. Rev. Lett.* **68** 1671
[16] Schroeder W U and Huizenga J R 1984 *Treatise of Heavy Ion Science* vol 2 ed D A Bromley (New York: Plenum) p 116
[17] Freiesleben H and Kratz J V 1984 *Phys. Rep.* **106** 1
[18] Krolas W 1996 *PhD Thesis* Institute of Nuclear Physics, Krakow, Report 1738
[19] Broda R *et al* 1998 *Acta Phys. Hung.* **7** 71
[20] Krolas W *et al* 2003 *Nucl. Phys.* A **724** 289
[21] Swiatecki W J 1972 *J. Phys. Colloq.* **33** C5–45
[22] Swiatecki W J 1995 private communication
[23] Cocks J F C *et al* 2000 *J. Phys. G: Nucl. Part. Phys.* **26** 23
[24] Motobayashi T *et al* 1995 *Phys. Lett.* B **346** 9
[25] Poves A and Retamosa J 1994 *Nucl. Phys.* A **571** 221
[26] Huck A *et al* 1985 *Phys. Rev.* C **31** 2226
[27] Fornal B *et al* 1994 *Phys. Rev.* C **49** 2413
[28] Fornal B *et al* 1997 *Phys. Rev.* C **55** 1
[29] Fornal B *et al* 2000 *Eur. Phys. J.* A **7** 147
[30] Scheit H *et al* 1996 *Phys. Rev. Lett.* **77** 3967
[31] Liang X *et al* 2002 *Phys. Rev.* C **66** 014302
[32] Ollier J *et al* 2003 *Phys. Rev.* C **67** 024302
[33] Ollier J *et al* 2005 *Phys. Rev.* C **71** 034316
[34] Broda R 2001 *Acta Phys. Pol.* B **32** 2577
[35] Broda R *et al* 2002 *Proc. 7th Int. Spring Seminar on Nucl. Phys. (Maiori, Italy, 2001)* ed A Covello (Singapore: World Scientific) p 195
[36] Janssens R V F *et al* 2002 *Phys. Lett.* B **546** 55
[37] Liddick S N *et al* 2004 *Phys. Rev. Lett.* **92** 072502
Liddick S N *et al* 2004 *Phys. Rev.* C **70** 064303
[38] Fornal B *et al* 2004 *Phys. Rev.* C **70** 064304
[39] Honma M *et al* 2002 *Phys. Rev.* C **65** 061301
[40] Fornal B *et al* 2005 *Phys. Rev.* C **72** 044315
[41] Broda R *et al* 2005 *Acta Phys. Pol.* B **36** 1343
[42] Pawlat T *et al* 1994 *Nucl. Phys.* A **574** 523
[43] Broda R *et al* 1995 *Phys. Rev. Lett.* **74** 868
[44] Grzywacz R *et al* 1998 *Phys. Rev. Lett.* **81** 766
[45] Pawłat T *et al* 1995 *Legnaro Nat. Lab. Annual Report* LNL INFN 095 7
[46] Wilson A N 1998 *Eur. Phys. J.* A **9** 183
[47] Broda R *et al* 1998 *Nuovo Cimento* A **111** 621
[48] Bosch U *et al* 1988 *Nucl. Phys.* A **477** 89
[49] Ishii T *et al* 2000 *Phys. Rev. Lett.* **84** 39
[50] Mayer R H *et al* 1992 *Z. Phys.* A **342** 247
[51] Mayer R H *et al* 1994 *Phys. Lett.* B **336** 308
[52] Daly P J *et al* 1995 *Phys. Scr.* T **56** 94
[53] Zhang C T *et al* 2000 *Phys. Rev.* C **62** 057305
[54] Zhang C T *et al* 1998 *Nucl. Phys.* A **628** 386
[55] Broda R *et al* 2004 *Eur. Phys. J.* A **20** 145
[56] Broda R *et al* 1999 *Phys. Rev.* C **59** 3071
[57] Daly P J *et al* 1999 *Phys. Rev.* C **59** 3066
[58] Blomqvist J 1999 *Acta Phys. Pol.* B **30** 697
[59] Khoo T L *et al* 1976 *Phys. Rev. Lett.* **37** 823
[60] Walker P M and Dracoulis G D 1999 *Nature* **399** 35
[61] Åberg S 1978 *Nucl. Phys.* A **306** 89
[62] Wheldon C *et al* 1998 *Phys. Lett.* B **425** 239
[63] Wheldon C *et al* 1999 *Eur. Phys. J.* A **5** 353
[64] Wheldon C *et al* 2000 *Phys. Rev.* C **62** 057301
[65] Chowdhury P *et al* 2001 *Nucl. Phys.* A **682** 65c

[66] Shestakova I *et al* 2001 *Phys. Rev.* C **64** 054307
[67] Schlegel C *et al* 2000 *Phys. Scr.* T **88** 72
[68] Pfützner M *et al* 2002 *Phys. Rev.* C **65** 064604
[69] Schramm M *et al* 1993 *Z. Phys.* A **344** 363
[70] Martin M J 1985 *Nucl. Data Sheets* **47** 797
[71] Broda R *et al* 1996 *Proc. Conf. on Nucl. Structure at the Limits (Argonne, IL)* ANL/Phy-97/1 276
[72] Wrzesiński J *et al* 2001 *Eur. Phys. J.* A **10** 259
[73] Schramm M *et al* 1992 *Z. Phys.* A **344** 121
[74] Wollersheim H J *et al* 1992 *Z. Phys.* A **341** 137
[75] Wrzesiński J and Broda R 2006 Private communication
[76] Rejmund M *et al* 1998 *Eur. Phys. J.* A **1** 261
[77] Rejmund M *et al* 1997 *Z. Phys.* A **359** 243
[78] Lane G J *et al* 2005 *Phys. Lett.* B **606** 34
[79] Fornal B *et al* 2003 *Phys. Rev.* C **67** 034318
[80] Lane G J *et al* 2001 *Nucl. Phys.* A **682** 71c
[81] Fornal B *et al* 1998 *Eur. Phys. J.* A **1** 355
[82] Rejmund M 1999 *PhD Thesis* GSI DISS 99–03
[83] Wrzesiński J *et al* 2004 *Eur. Phys. J.* A **20** 57
[84] Fornal B *et al* 2001 *Phys. Rev. Lett.* **87** 212501
[85] Rejmund M *et al* 2000 *Eur. Phys. J.* A **8** 161
[86] Ward D *et al* 1996 *Nucl. Phys.* A **600** 88
[87] Wiedenhöver I 1999 *Phys. Rev. Lett.* **83** 2143
[88] Cocks J F C *et al* 1997 *Phys. Rev. Lett.* **78** 2920
[89] Cocks J F C *et al* 1999 *Nucl. Phys.* A **645** 61
[90] Fernandez-Niello J *et al* 1991 *Nucl. Phys.* A **531** 164
[91] Ward D *et al* 1983 *Nucl. Phys.* A **406** 591
[92] Bonin W *et al* 1985 *Z. Phys.* A **322** 59
[93] Butler P A and Nazarewicz W 1995 *Rev. Mod. Phys.* **68** 349
[94] McDonald R J *et al* 1982 *Nucl. Phys.* A **373** 54
[95] Pacheco A J *et al* 1983 *Nucl. Phys.* A **397** 313
[96] Lee I Y 1997 *Acta Phys. Pol.* B **28** 257
[97] Simon M W *et al* 2000 *Nucl. Instrum. Methods* A **452** 205
[98] Regan P H *et al* 2003 *Phys. Rev.* C **68** 044313
[99] Valiente-Dobon J J *et al* 2004 *Phys. Rev.* C **69** 024316
[100] Regan P H *et al* 2004 *Laser Phys. Lett.* **1** 317
[101] Kulp W D *et al* 2005 *Phys. Rev.* C **71** 041303
[102] Hua H *et al* 2004 *Phys. Rev.* C **69** 014317
[103] Stefanini A *et al* 2002 *Nucl. Phys.* A **701** 109c
[104] Gadea A *et al* 2004 *Eur. Phys. J.* A **20** 193
[105] Gadea A *et al* 2005 *J. Phys. G: Nucl. Part. Phys.* **31** S1443
[106] Savajols H 2003 *Nucl. Instrum. Methods* B **204** 146